Review of selective laser melting : materials and applications

Yap, Chor Yen; Chua, Chee Kai; Dong, Zhi Li; Liu, Zhong Hong; Zhang, Dan Qing; Loh, Loong Ee; Sing, Swee Leong

2015

Yap, C. Y., Chua, C. K., Dong, Z. L., Liu, Z. H., Zhang, D. Q., Loh, L. E., & Sing, S. L. (2015). Review of selective laser melting : materials and applications. Applied Physics Reviews, 2(4), 041101-. doi:10.1063/1.4935926

https://hdl.handle.net/10356/87847

https://doi.org/10.1063/1.4935926

APPLIED PHYSICS REVIEWS—FOCUSED REVIEW

Review of selective laser melting: Materials and applications

C. Y. Yap,[1,2,a)] C. K. Chua,[1,b)] Z. L. Dong,[3,c)] Z. H. Liu,[1,d)] D. Q. Zhang,[1,e)] L. E. Loh,[1,f)] and S. L. Sing[1,g)]
[1]*Singapore Centre for 3D Printing, School of Mechanical and Aerospace Engineering, Nanyang Technological University, 50 Nanyang Avenue, Block N3.1 - B2c - 01, Singapore 639798*
[2]*Energy Research Institute @ NTU, Interdisciplinary Graduate School, Nanyang Technological University, 50 Nanyang Avenue, Block S2 - B3a - 01, Singapore 639798*
[3]*School of Materials Science & Engineering, Nanyang Technological University, 50 Nanyang Avenue, Block N4.1, Singapore 639798*

(Received 14 July 2015; accepted 23 October 2015; published online 9 December 2015)

Selective Laser Melting (SLM) is a particular rapid prototyping, 3D printing, or Additive Manufacturing (AM) technique designed to use high power-density laser to melt and fuse metallic powders. A component is built by selectively melting and fusing powders within and between layers. The SLM technique is also commonly known as direct selective laser sintering, LaserCusing, and direct metal laser sintering, and this technique has been proven to produce near net-shape parts up to 99.9% relative density. This enables the process to build near full density functional parts and has viable economic benefits. Recent developments of fibre optics and high-power laser have also enabled SLM to process different metallic materials, such as copper, aluminium, and tungsten. Similarly, this has also opened up research opportunities in SLM of ceramic and composite materials. The review presents the SLM process and some of the common physical phenomena associated with this AM technology. It then focuses on the following areas: (a) applications of SLM materials and (b) mechanical properties of SLM parts achieved in research publications. The review is not meant to put a ceiling on the capabilities of the SLM process but to enable readers to have an overview on the material properties achieved by the SLM process so far. Trends in research of SLM are also elaborated in the last section. [http://dx.doi.org/10.1063/1.4935926]

TABLE OF CONTENTS

[a)]cyap001@e.ntu.edu.sg
[b)]Author to whom correspondence should be addressed. Electronic mail: mckchua@ntu.edu.sg. Ph. +65 6790 5486
[c)]zldong@ntu.edu.sg
[d)]azhliu@ntu.edu.sg
[e)]zhangdq@ntu.edu.sg
[f)]leloh1@e.ntu.edu.sg
[g)]sing0011@e.ntu.edu.sg

I. INTRODUCTION

A. Background on selective laser melting

Selective Laser Melting (SLM) is an additive manufacturing process developed by Dr. M. Fockele and Dr. D. Schwarze of F & S Stereolithographietechnik GmbH, with Dr. W. Meiners, Dr. K. Wissenbach, and Dr. G. Andres of Fraunhofer ILT to produce metal components from metallic powders. It is a powder bed fusion process that uses high intensity laser as an energy source to melt and fuse selective regions of powder, layer by layer, according to computer aided design (CAD) data. The patent for this technology was first applied in 1997 to the German Patent and Trade Mark Office and published in 1998.[1] In 2001, patent was also filed by Das and Beaman based on their pioneering works in direct selective laser sintering (SLS).[2]

The SLM process consists of a series of steps from CAD data preparation to removal of fabricated component from the building platform. Before the CAD data are uploaded to the SLM machine for production of components, the STereoLithography (STL) files have to be processed by software, such as Magics, to provide support structures for any overhanging features and to generate slice data for laser scanning of individual layers. The building process starts with laying a thin layer of metal powder on a substrate plate in a building chamber. After the powder is laid, a high energy density laser is used to melt and fuse selected areas according to the processed data. Once the laser scanning is completed, the building platform is lowered, a next layer of powder is deposited on top and the laser scans a new layer. The process is then repeated for successive layers of powder until the required components are completely built.[3] Process parameters, such as laser power, scanning speed, hatch spacing, and layer thickness, are adjusted such that a single melt vector can fuse completely with the neighbouring melt vectors and the preceding layer. Once the laser scanning process is completed, loose powders are removed from the building chamber and the component can be separated from the substrate plate manually or by electrical discharge machining (EDM). Besides the data preparation and removal of fabricated component from the building platform, the entire process is automated. Figure 1 illustrates the concept of the SLM building process.

During the SLM process, the building chamber is often filled with nitrogen gas or argon gas to provide an inert atmosphere to protect the heated metal parts against oxidation. Furthermore, some of the SLM machines are capable of providing pre-heating either to the substrate plate or the entire building chamber. The thickness of the layer usually ranges from 20 to 100 μm. This is chosen as a balance between achieving fine resolution and allowing for good powder flowability.[4] Powders with larger particulate sizes result in poor resolution and build tolerance, while smaller powders have the tendency to agglomerate together easily due to van der Waals forces, resulting in poor powder flowability and hence poor powder deposition.

Literatures have shown that SLM is capable of fully melting the powder material, producing fully dense near net-shape components without the need for post-processing, other than the removal of parts and supports from substrate plate. This makes SLM a superior Additive Manufacturing (AM) process compared to SLS, which binds powder materials via solid state sintering or melting of binding agents, resulting in parts with high porosity and low strength. Post-processing, such as heat treatment and material infiltration, usually needed to improve the SLS components, is time consuming and significantly lengthens the process. In SLM, full melting of powder is achieved by the use of high-intensity laser and binder materials are not required, eliminating the need for the above-mentioned downstream processes. The current SLM technology provides improvements in product quality, processing time, and manufacturing reliability compared to binder-based laser sintering AM processes.

In addition to direct manufacturing, SLM has also been adapted to perform repairs on damaged components. The Direct Digital Manufacturing Lab at Georgia Tech has developed Scanning Laser Epitaxy (SLE) for additive repair of

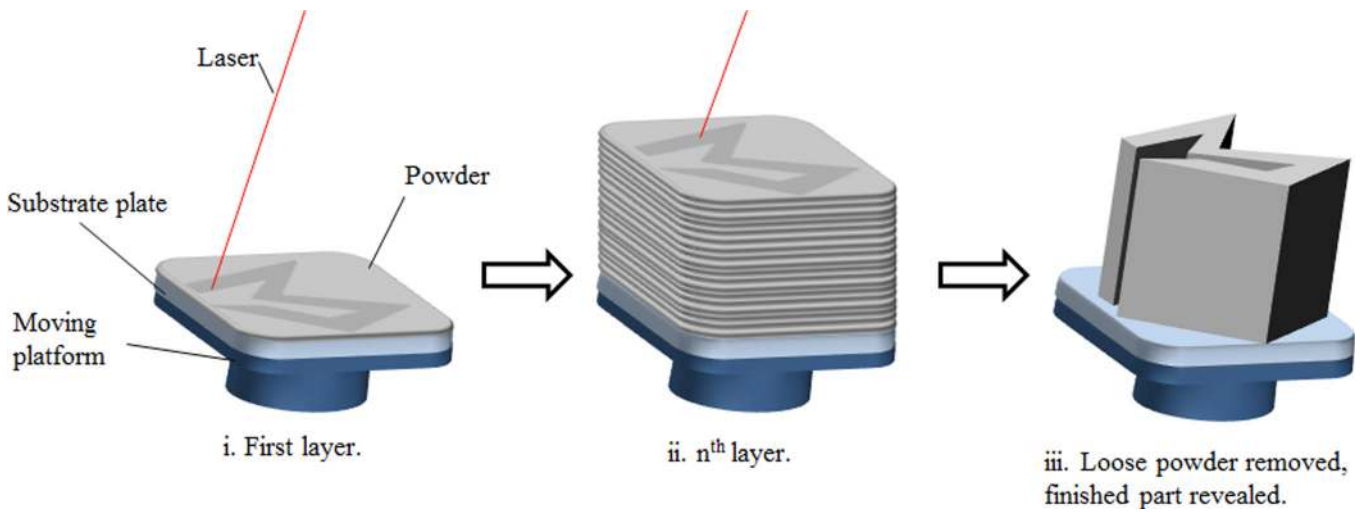

FIG. 1. Concept of SLM process. (i) High-power laser melts selective areas of the powder bed. (ii) Process is repeats for successive layers. (iii) Loose powder removed and finished part revealed.

nickel-based alloys CMSX-4,[5,6] Rene 80,[7] and IN100.[8] SLE requires a small amount of powder for repair, enough to cover the surface of the damaged part up to 2 mm in powder thickness. A high power Nd:YAG laser is then deployed to melt the powder material, covering cracks and holes in the damaged component.

Other additive manufacturing processes, such as LaserCusing and Direct Metal Laser Sintering (DMLS), are essentially the same as SLM. In order to keep this review focused, publications in which manufacturing processes involve complete melting of powder bed by laser will be included and SLM will be the term used to represent these processes.

B. Scope

This review first presents some of the physical phenomena commonly mentioned in SLM literatures. Sections II–V are organized according to the materials used, mainly metals, ceramics and composite materials. Under the category of metals, the materials are further divided into "steel and iron-based alloys," "titanium and its alloys," "Inconel and nickel-based alloys," and "other metals."

Under each material group, applications of the SLM materials are elaborated. Moreover, the best properties achieved, such as highest relative density, highest strength, highest hardness, and lowest surface roughness, are also compiled and tabulated for readers to have a quick glance and for ease of comparison. Relative density of SLM parts is often examined to determine if all the powders in the component have been melted. Strength and hardness are basic material properties that can be compared to cast parts to indicate the suitability of SLM parts for various applications. Surface roughness determines if post-processes, such as grinding and polishing, are required. However, it is to note that these figures do not show the limits of the technology. Instead, they are meant to demonstrate the progress of research in the SLM process. Section VI illustrates the trend of research in SLM and its future outlook.

II. PHYSICAL PHENOMENA IN SLM

SLM involves the heating and melting of powder material with laser beam and rapid solidification of the melted material to form the desired component. There are several physical phenomena that are important to the process, such as the absorptivity of the powder material to laser irradiation, the balling phenomena that disrupt the formation of continuous melts, and the thermal fluctuation experienced by the material during the process that can lead to crack formation and component failure. In this section, investigations on these aspects of SLM are presented to shed light on the physics involved in the SLM process. Literatures on simulation and numerical analysis of SLM are beyond the scope of this review.

A. Laser and material interaction

SLM was designed with the intent to heat up and melt metallic materials. The laser systems for SLM progressed from CO_2 laser ($\lambda \approx 10.6\,\mu$m), adapted from the selective laser sintering process to Nd:YAG fibre laser ($\lambda \approx 1.06\,\mu$m) and subsequently to Yb: YAG fibre laser. This is due to the higher absorptance of metallic powders to radiation of such wavelengths in the infrared region. Furthermore, compared to the commonly used Nd:YAG crystal, Yb:YAG crystal has a larger absorption bandwidth to reduce thermal management requirements for diode lasers, a longer upper-state lifetime, and a lower thermal loading per unit pump power. Yb:YAG crystal is expected to replace Nd:YAG crystal for high power diode-pumped lasers and other potential applications. The advancements in laser technology will continue to bring about higher energy efficiency to the SLM process.

In SLM, laser power, scanning speed, hatch spacing, and layer thickness are the common process parameters adjusted to optimize the process. Figure 2 provides an illustration of these process parameters commonly studied in SLM. Together with the absorptance of powders to the laser irradiation, these parameters affect the volumetric energy density that is available to heat up and melt the powders. When heating and melting occurs, heat capacity and latent heat have to be taken into account. These are heavily dependent on the material and proportional to the mass to be melted. Insufficient energy, usually a combination of low laser power, high scanning speed, and large layer thickness, often results in balling due to lack of wetting of molten pool with the preceding layer.[9] However, high laser and low scanning speed may result in extensive material evaporation and the keyhole effect.[10] In addition, poor hatch spacing often results in regular porosity in built parts as adjacent melt lines do not fuse together completely. Moreover, vaporization in SLM often results in condensation of volatilized materials on the laser window, disrupting the delivery of laser power.[11] Hence, suitable combination of laser power, scanning speed, hatch spacing, and layer thickness is essential for SLM processing to successfully build near full-density parts.

One of the integral aspects of laser-material interaction is the absorption of energy by the powder. The absorptance, defined as the ratio of the energy flux absorbed by the

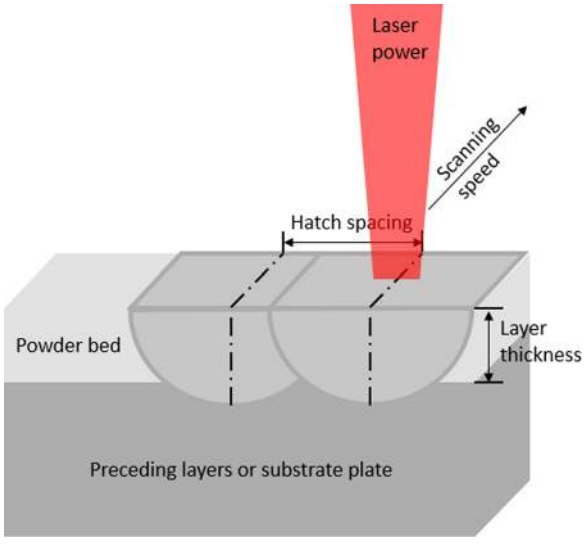

FIG. 2. SLM process parameters: laser power, scanning speed, hatch spacing, and layer thickness.

material to the energy flux incident upon the material, affects the energy efficiency of the SLM process. It can even determine the feasibility of processing materials with a specific laser. Physicists have studied the absorptivity of various materials to irradiation of different wavelengths. However, few of these works are done with powder materials. In SLM, laser is irradiated onto a thin powder bed and the absorptivity of powder materials to laser irradiation can be drastically different from their corresponding bulk materials. Tolochko *et al*. investigated the absorptance of powder materials to infrared irradiation of CO_2 laser (wavelength, $\lambda = 10.6\,\mu$m) and Nd-YAG laser ($\lambda = 1.06\,\mu$m).[12] In comparison to the absorptance of bulk materials with smooth surfaces, powder materials have significantly higher absorptance regardless of the wavelength of irradiation. For instance, at $\lambda = 1.06\,\mu$m, the absorptance of titanium bulk material is 30%,[13] while that of titanium powder is 77%.[12]

The high absorptance of powder material can be explained by the multiple reflections of the laser beam in the powder bed, which also result in higher optical penetration depth.[13] Wang *et al*. studied this phenomenon with a 2D optical ray tracing model, taking into account the geometry and structure of the powder.[14] In an attempt to model the SLM process, Gusarov and Kruth compared the effective absorptance of powder bed with the absorptance of bulk material and match experimental data with both the isotropic specular reflection model and diffuse reflection model.[15] The model, substantiated by the data, allows for prediction of the absorptance of powder bed based on that of bulk material Figure 3. Their work provide models to calculate the ratio of the total absorption with respect to the material absorption and to predict the optimal laser parameters with which to process a particular material.

In addition to the studies on absorptance of irradiation with various materials, there are also research works that

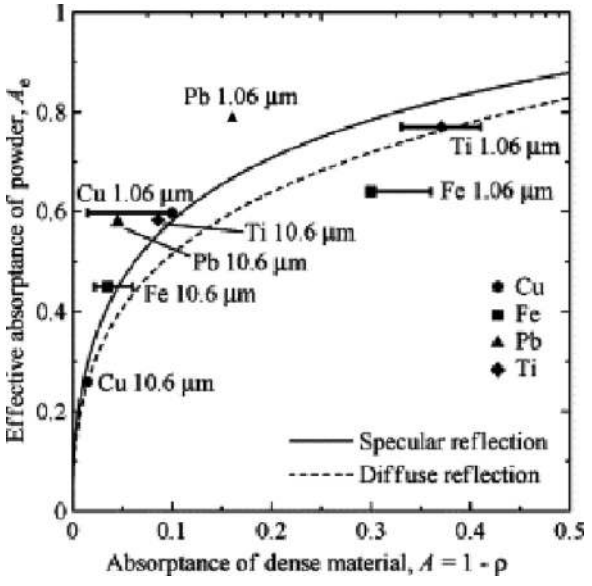

FIG. 3. Effective absorptance of powder bed vs absorptance of bulk material; with experiment data (data points) and prediction by isotropic specular reflection model (solid line) and diffuse reflection model (dotted line).[15] Reproduced with permission from A. V. Gusarov and J. P. Kruth, Int. J. Heat Mass Transfer **48**, 3423–3434 (2005). Copyright 2005 Elsevier.

examine the effects of the energy distribution profile of lasers and the difference between pulsed and continuous lasers. Loh *et al*. used AA6061, an aluminium alloy, to examine the different effects of Gaussian beam profile and uniform beam profile in SLM. Their investigation found that a uniform beam laser was able to achieve a larger melt width for similar amount of melt penetration. Hence, a uniform beam laser could be used to increase the productivity of SLM by reducing the hatch spacing in the process.[16] Furthermore, a simplified modelling of the SLM process based on AA6061 has also been developed. The numerical model takes into account the volumetric shrinkage and material loss due to vaporization of the process.[17]

Mumtaz and Hopkinson[18] reported a study on SLM of Inconel 625 with pulsed laser. Using the pulsed laser allowed them to add another dimension of control to the SLM process as the laser pulse could be adjusted for different pulse durations, frequencies, and pulse shapes. Their results showed that a ramp-down pulse shape lowered the surface roughness of the top surface but was detrimental to that of the side surfaces. However, the effects of pulse shape on other properties, such as hardness and strength, were yet to be tested. Moreover, it is noted that the scanning speed of this system was limited to 400 mm/s, possibly restricted by the highest frequency and longest pulse duration attainable for a continuous melt track.

In addition to laser parameters, powder size and powder distribution also have effects on the required process parameters. However, there are few published works on this. A study by Bourell *et al*. suggests that smaller 316L stainless steel powders with D_{50} of 15 μm and 28 μm require a lower energy density to achieve 99.0% density than steel powders with D_{50} of 38 μm.[19] Another study by Liu *et al*. confirmed that existence of smaller powders allows high density parts to be built with lower laser energy intensity and better surface finish.[20] However, powders with narrow range of particle size flow better and generate parts with higher strength and hardness. These studies only showed some of the possible effects of powder size and size distribution on the required SLM processing parameters. The effects of powder size or size distribution on the processing envelope of different materials are still unclear as they have yet to be investigated independently. Moreover, universality of their effects across different materials is also not established.

B. Balling

Balling is a particular phenomenon in SLM where molten metal forms spheroidal beads due to insufficient wetting of the preceding layer and surface tension.[11,21] It obstructs the formation of continuous melt lines, forming rough and bead-shaped surfaces. In more severe cases, balling may aggravate in subsequent layers and cause the SLM process and jam the powder coating mechanism with large metallic beads that extend above the powder bed (Figure 4).[9]

In Li *et al*.'s study of the balling phenomenon, it is shown that balling could be reduced significantly by keeping oxygen level at 0.1%, applying a combination high laser power and low scanning speed or applying re-scanning of

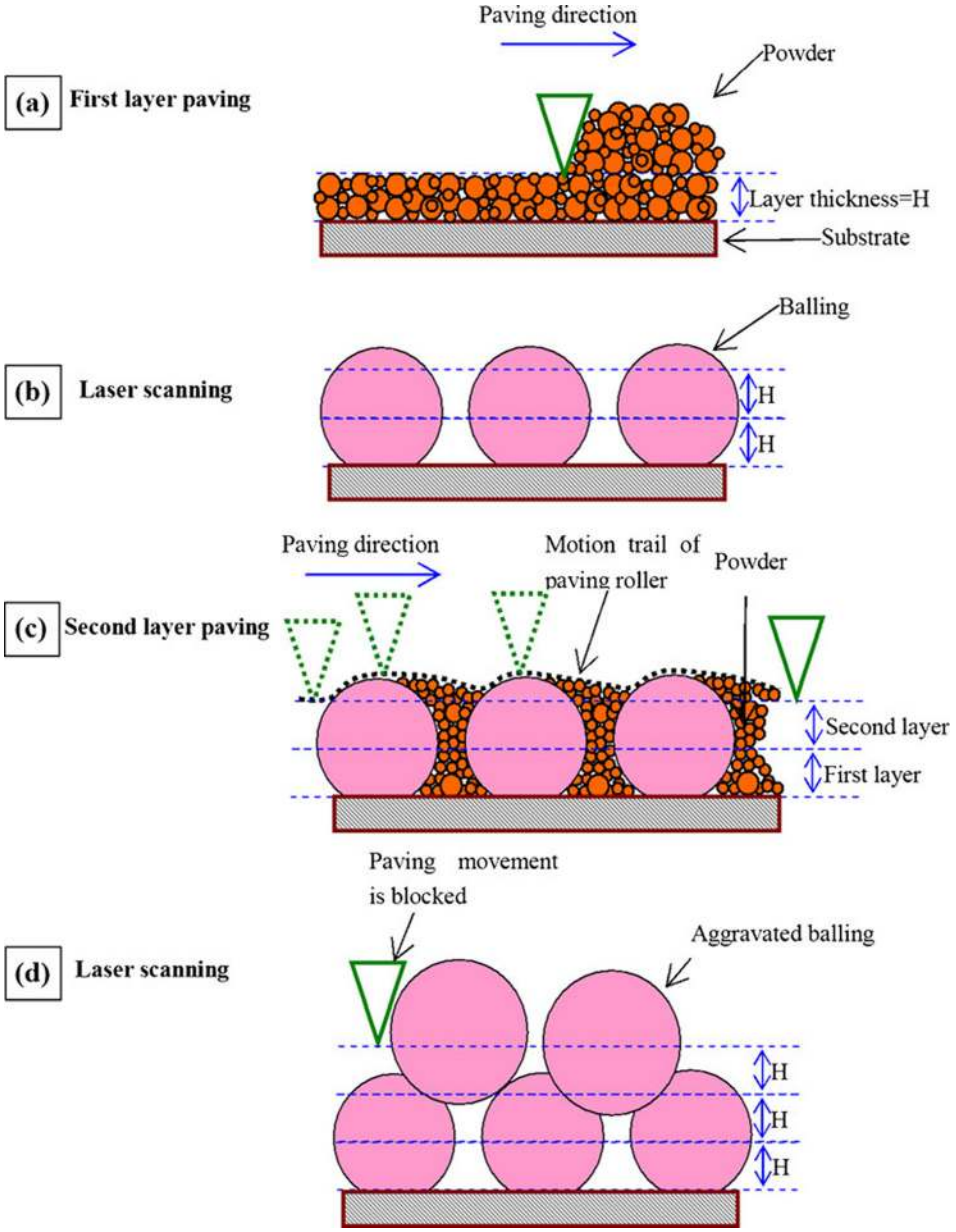

FIG. 4. Aggravation of balling that jams powder coating mechanism in SLM.[9] Reproduced with permission from R. Li *et al.*, Int. J. Adv. Manuf. Technol. **59**, 1025–1035 (2011). Copyright 2011 Springer.

laser.[9] Das and Kruth *et al.* explained that an oxide film on the preceding layer impedes interlayer bonding and leads to balling as liquid metals generally do not wet oxide films in the absence of a chemical reaction.[11,22] In combination with thermal stresses, poor interlayer bonding also leads delamination. Hence, lowering the oxygen level during the process and introducing repeat exposure of laser to break up the oxide films are ways to minimise the occurrence of balling.

C. Thermal fluctuation and its effects

The materials experience varying degrees of thermal fluctuation during the SLM process. This causes residual stress on the components built, as explained by Kempen *et al.* with the temperature gradient mechanism.[23] This mechanism can lead to crack formation and delamination of parts as shown in Figure 5. A recent study has also compared the temperature profile in SLM of 316 L stainless steel and Ti-6Al-4V during SLM and it shows that thermal gradient is more pronounced in Ti-6Al-4V due to the difference in thermal properties.[24]

Shiomi *et al.* addressed the issue of residual stresses and methods of reducing them in SLM components made of chrome molybdenum steel mixed with nickel and copper phosphate powders.[25] It was found that heat treatment of such SLM components at 600 °C–700 °C for 1 h reduced residual stress by 70%; re-scanning of laser with the same parameters as the SLM forming process reduced residual stress by 55%; and heating of powder bed to 160 °C resulted in a 40% reduction. This paper gave three main methods to reducing them and these methods have since been repeatedly examined in various research works with regards to the SLM process.

More recently, Yasa *et al.* introduced "sectorial scanning" as a scanning strategy in SLM.[26] This strategy breaks down a layer into small square grids and neighbouring grids are scanned perpendicular to one another. It was found

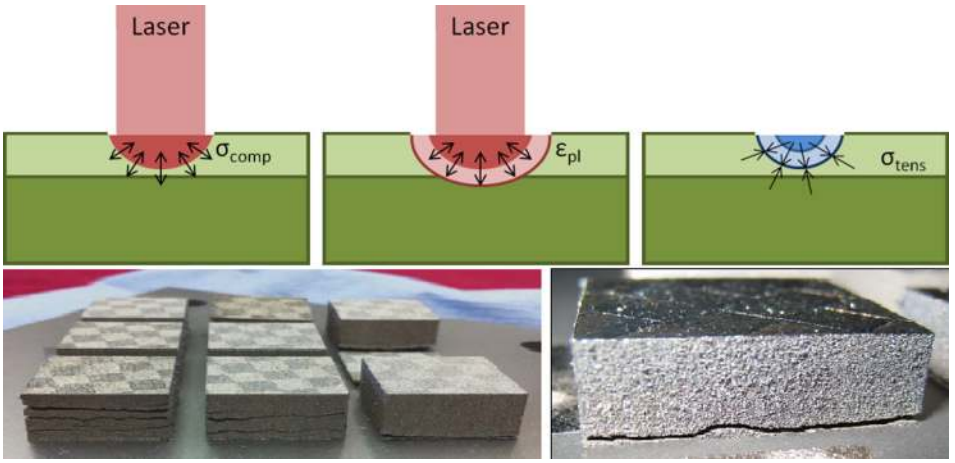

FIG. 5. Temperature gradient mechanism (top) leading to crack formation and delamination (bottom).[23] Reproduced with permission from K. Kempen *et al.*, Solid Freeform Fabrication Symposium Proceedings (2013). Copyright 2013 The University of Texas at Austin.

that "sectorial scanning" is able to reduce the residual stress significantly. This strategy is now available in processing software, such as Autofab or SLM Build Processor and is known as chessboard strategy.

The problem of crack formation and delamination is especially prevalent in ceramic materials. Ceramics require very high melting temperatures and have very low thermal conductivity, resulting in very high thermal gradient during the process. Combined with its low fracture toughness, ceramics present a difficult challenge for researchers to produce a crack-free part via SLM. In order to tackle the problem, Hagedorn's research group made two approaches.[27] Firstly, they used a eutectic mixture of alumina and zirconia so that the required melting temperature was lowered to 1860 °C. Secondly, a secondary laser was used to preheat the surface powder to temperatures above 1600 °C as the primary laser melted the selected area according to CAD data as shown in Figure 6. These approaches directly lowered the temperature fluctuation experienced by the SLM part during the process and allowed the finished parts to be crack-free. The inherent issues of balling, residual stress, and crack formation can be mitigated by combination of preheating, selecting the right scanning strategy and parameters, and post-process heat treatment.

III. METALS IN SLM AND THEIR APPLICATION

Most of the SLM research revolves around three types of metals: iron, titanium, and nickel. These metals were selected due to their widespread application and their material cost. As research progressed, many other metals, such as aluminium, copper, magnesium, and tungsten, have also been tested for SLM and they are discussed in Section III D.

A. Steel and iron-based alloys

From 2003 to 2013, there are more than 100 publications on the SLM of steel or ferrous alloys alone. The main advantage of processing metals with SLM lies with the flexibility of SLM to fabricate components with structured porosity. This enables product developers to harness the toughness of steel and add considerable weight-saving to their design to compensate for steel's relatively high density.

Most of the research publications on SLM of ferrous metals are based on 316L stainless steel. Abe *et al.* ran preliminary tests on this material in 2001 but it was not successful due to balling effects.[28] The first paper that reported successful SLM of 316L stainless steel was made by Jandin *et al.* In their study, ytterbium fibre laser with a wavelength of 1065 nm was used to process the 316L stainless steel powder. The experiment showed that low laser power and high scanning speed caused incomplete melting of the powder material and resulted in high porosity components. This can be improved by increasing the laser power, decreasing the scanning speed, or both.[29] However, it was not until 2010 that Tolosa *et al.* achieved 99.9% relative density with SLM of 316L stainless steel powder.[30]

Research group led by Childs from University of Leeds first reported investigation of M2 high speed steel (tool steel), H13 tool steel, and 314S stainless steel in 2004. They

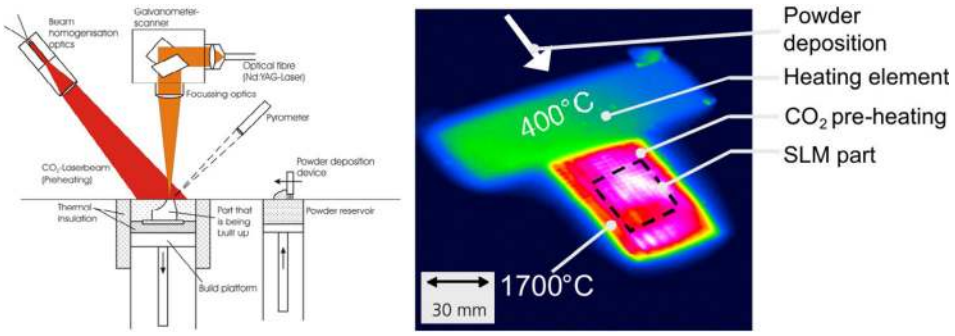

FIG. 6. Preheating mechanism with CO_2 laser, by Fraunhofer ILT.[27] Reproduced with permission from Y.-C. Hagedorn *et al.*, Phys. Proc. **5**, 587–594 (2010). Copyright 2010 Elsevier.

examined the melt track in the SLM process through modelling[31] and experiments[32] and showed that a combination of high laser power and low scanning speed produces stable melt tracks beneficial for the production of fully dense components. The process envelopes for a stable continuous melt track were mapped out for these materials and the maximum achievable scanning speed was just 15 mm/s. The group went on to examine single layer scanning of H13 by a raster-scanning strategy.[33] Later, Badrossamay and Childs[34] continued their studies on SLM to include M2 tool steel and 316L stainless steel. Both their experimental and simulation results showed that thermal history of the process affects the amount of powder melted under laser radiation. However, it is to note that a CO_2 laser, instead of the Nd:YAG laser commonly used now, with a maximum power of 200 W was used in their experiments and scanning speeds were as low as 0.5 mm/s.

Furthermore, by exploiting the flexibility of the SLM process, Jerrard *et al*. have investigated the SLM of 316L stainless steel and 17-4 PH stainless steel powder mixture.[35] Their work showed that hardness and magnetic adherence of the SLM component can be adjusted by varying the compositional ratio of the contents. Hence, new grades of steel can be produced via SLM to tailor properties to specific functions and needs.

Different variants of steel have also been investigated for processing by SLM. These include Inox904L stainless steel, AISI Maraging 300 steel, 15-5 and 17-4 precipitation hardening steel, H20 tool steel, and tool steel X110CrMoVAl 8-2. Besides steels, iron-based alloys and intermetallics, such as Fe-Ni, Fe-Ni-Cu-P, Fe-Ni-Cr, Fe-Al, and Fe-Cr-Al alloys, have also been tested with SLM although publications of such materials are much fewer. Thus far, these research works mainly examined the suitable processing parameters to achieve fully dense components with these materials and their resultant microstructures.

1. Applications

There are many applications of SLM steel materials, depending on the properties, such as strength, ductility, and biocompatibility. As the current SLM process is expensive compared to most conventional manufacturing methods, proposed applications are in high value-added industries, such as medicine. The unique ability of SLM to produce metallic parts with complex geometries directly also allows researchers to look into applications where conformal cooling channels are required for tooling and lightweight structures for the aerospace and automotive industries.

a. Medical and dental applications. Yadroitsev *et al*. presented SLM as a "promising direction to solve challenging medical problems."[36] The main benefit of SLM in this field is that the products from SLM can be customized to suit individual needs at virtually no customization cost and fully functional parts can be built directly.

Kruth *et al*.[37] published a biocompatible metal framework for dental prostheses and Wehmoller *et al*.[38] reported body implants of cortical bone, mandibular canal segment, and support structures or tubular bone made from SLM 316L stainless steel. Chen *et al*.[39] and Bertrand and Smurov[40] separately reported SLM denture frameworks with the same material. Yang *et al*.[41] investigated the optimization of building accuracy and density of orthodontic products using a self-developed SLM machine and they were able to achieve the required surface quality and mechanical properties. Li *et al*.[42] studied the possibility of making SLM 316L stainless steel parts with gradient porosity where the dense portion is designed for strength and the porous portion is designed to enhance tissue growth in biocompatible implants.

The feasibility of using SLM steel parts for biomedical applications has been confirmed by Bibb *et al*.[43] The paper presented four different case studies on successful surgical guides in different maxillofacial (jaw and face) surgeries. However, there has not been any published study on implants made from SLM steel parts.

b. Heat exchangers. As do most AM technologies, SLM provides the freedom of design to make conformal cooling channels and this is especially applicable to injection moulding. Smurov's research group demonstrated a mini pump die and small parts with conformal cooling channels,[44] displaying the ability of SLM to create small and complex parts with Inox904L steel. The research contributed to the fabrication of the diverter thimbles in the cooling system of the International Thermonuclear Experimental Reactor (ITER).[45] In a similar manner, Garcia *et al*.[46] incorporated spiral conformal cooling channels for injection moulding and found that both cycle time and part quality were dramatically improved. Brandner *et al*.[47] showed that SLM can produce micro-scale devices with wall thickness of about 100 μm which enables the fabrication of micro-scale structures. Wong *et al*.[48] further investigated the effectiveness of complex shape heat exchangers manufactured via SLM and the effects on the heat exchange and fluid pressure. Beal *et al*.[49] built functionally graded injection mould and investigated the heat conductivity and heat capacity of the parts. Wang *et al*.[50] also fabricated mould inserts with conformal cooling channels using SLM. Their works demonstrated that different cooling rates can be achieved in the mould using cooling channels.

SLM of ferrous intermetallics, such as Fe-Al, has also been studied for such application.[51] Fe-Al has high strength to weight ratio, excellent resistance to oxidation, wear and corrosion, and it is often used in high temperature systems, such as furnace fixtures, heat exchange piping, turbine blades in jet engines, etc.

c. Light weight structures. The ability of SLM to create complex lattice structures has also led to research in cellular lightweight structures. The structure contains repeated three-dimensional single cells. These structures enable engineers to easily alter the density and strength of the overall product according to needs. The first paper on SLM of steel lightweight structures was reported by Santorinaios *et al*.[52] on the crush behaviour of such structures. Following this, there

have been more research works that investigated the quasi-static and blast response,[53] compressive properties,[54] shock response,[55] failure mechanism[56] of the steel lattice structures. In most of these works, 316L stainless steel was used. The cellular lattice structure can be deployed as the core of a sandwich structure which makes it lightweight and strong. However, few investigations of the sandwich structure with SLM steel lattice core have been published. Only Shen *et al.*[57] studied the compressive behaviour and failure mechanisms of the sandwich structure and Mines *et al.*[58] examined its drop-weight impact behaviour.

Besides cellular lattice structures, honeycomb-like structures have also been studied. Rehme and Emmelmann[59] investigated the SLM steel honeycomb structure with negative Poisson's ratio, where the material is required to show high compressibility and minimum resistance to compression. This structure can be applied as crash impact absorbers in bullet proof vest and artificial intervertebral discs.

Usually, the wall or strut thicknesses of these lattice structures is in the range of 100 μm. This is due to the limitations of laser spot diameter and the resultant melt profile created by the laser. However, Shen's group managed to create micro-scale pores with walls thinner than 1 μm.[60] This was achieved by adding 0.1 wt. % of H_3BO_3 and KBF_4. The pores and walls were created as a result of the gas generated by the additives. Similar results were also achieved with NH_4HCO_3 as additives.[61] The drawback is that the pores and wall structures cannot be controlled.

d. Other applications. In other SLM applications of steel or iron-based alloys, Milovanovic *et al.*[62] made a case study for AM of tyre tread ring segment mould with H20 tool steel. Feuerhahn *et al.*[63] studied the SLM of a high hardness tool steel X110CrMoVAl 8-2 for applications in micro-tooling. Their studies showed that SLM was able to produce a part with very high hardness with fine structure at the same time. This cannot be achieved by conventional methods, such as spray forming or forging. Production of fine-structured porous stainless steel filter elements by SLM was studied by Yadroitsev *et al.*[64]

2. Properties

a. Relative density. Relative density is often used as an indicator of the quality of the SLM parts. Relative density is the ratio of the density attained with SLM and the theoretical density of the bulk material. The theoretical density can be calculated from the atomic weight and crystal structure of the material. One may also refer to the ASM International material data sheet for the materials' densities. Most of the SLM steel or iron-based materials have reported relative densities above 90%. Table I summarizes the reported maximum density of the various SLM steel materials.

b. Strength. Steel is often used because of its strength. Hence, the engineering strength of SLM steel parts is of paramount importance for their respective applications. It is often reported that SLM steel components are stronger but less malleable compared to their cast counterparts. This is generally attributed to the nature of the SLM process, where very small amount of material is melted at a time and rapid solidification takes place. This results in a more uniform microstructure throughout the part. For alloys, the segregation of alloying elements takes place in a much smaller scale. Chemical composition is more uniform throughout the part, resulting in higher strength that cast parts.[77] This phenomenon is common for SLM materials.

TABLE I. Highest reported relative density of SLM steel and iron-based alloys.

Material	Highest relative density, %	References
Fe	99.00	65
Fe + 0.8% C	93.00	66
Fe-Al intermetallics	98.00	67
Fe_3Al	99.50	68
Fe-Ni	98.00	69
Fe-Ni-Cr	99.50	69
Fe-Ni-Cu-P	97.50	70
304L stainless steel	92.00	71
316L stainless steel	99.90	30
316L stainless steel	99.95 (laser remelting)	72
H13 tool steel	90.00	73
H20 tool steel	99.50	62
M2 high speed steel	97.00	74
AISI Marage 300 steel	99.99	75
Ultra high carbon steel	92.00	76

The table below shows the highest reported ultimate tensile strength (UTS) for each bulk material, along with their respective yield strength (YS) and elongation. It is noted that some research groups may not follow the ASTM E8 standard for tensile test of metallic materials. For instance, Guan *et al.*[78] used Chinese GB/T 228–2002 standard for their test on SLM 304 stainless steel. The annealed material UTS, available from ASM International, is listed on the right column for readers to have a point of reference. The reported strengths of lattice/cellular structures are not in Table II as they are dependent on design and can be tailored according to applications.

c. Surface roughness. One of the limitations of the SLM process is the surface roughness and it is common to achieve roughness of about 20 μm. Post processing, such as sand-blasting, shot-peening, or manual grinding is often needed to achieve a smooth and shiny surface with the exception for 316L stainless steel. Reported surface roughness of steel and iron-based alloy components made via SLM is shown in Table III.

d. Micro-hardness. Micro-hardness is important for tooling purposes. Table IV shows the highest reported micro-hardness of the various SLM steels and ferrous alloys. There are many different tests available for hardness and the results were converted to the HV scale in this review for comparison.

TABLE II. Highest reported tensile strengths of SLM steel and iron-based alloys.

Material	UTS (MPa)	YS (MPa)	Elongation (%)	References	Material UTS (MPa)
Fe	411.5	305.3	…	65	225
Fe-Ni	600	…	…	69	…
Fe-Ni-Cr	1100	…	…	69	…
Fe-Ni-Cu-P	505	425	…	70	…
15-5 PH steel	1450	1297	12.53	79	1317
15-5 PH steel	1470	1100	15.00	80	1317
304 stainless steel	717	570	42.80	78	579
316L stainless steel	760	650	30.00	19	558
Maraging steel	1290	1214	13.30	81	1930

TABLE III. Lowest reported surface roughness values of SLM steel and iron-based alloys.

Material	Surface roughness, R_a (μm)	References
Fe-Ni	10	69
Fe-Ni-Cr	10	69
304L stainless steel	25.7	71
316L stainless steel	5.82	82
316L stainless steel	5.00 (sand blasting)	19
316L stainless steel	2.00 (laser re-melting)	72
H20 tool steel	3.78 (shot-peening)	62
Ultra high carbon steel	18.0	76

B. Titanium and its alloys

In the last decade, the number of publications of SLM of titanium is second to that of steel. Almost all of these papers are based on commercially pure titanium (cpTi) or Ti-6Al-4 V alloy (Ti64). Titanium in the liquid state is highly reactive and sensitive to oxygen, nitrogen, hydrogen, and carbon, making it difficult for conventional processes, such as casting. In the SLM process, an inert gas, such as argon, is used to flush out atmospheric air and provide a layer of protective gas. Moreover, small localized heating and rapid cooling in SLM reduce the pick-up of interstitial elements, such as hydrogen, carbon, and oxygen. Other titanium based alloys, such as Ti-6Al-7Nb, Ti-24Nb-4Zr-8Sn, Ti-13Zr-Nb, and Ti-13Nb-13Zr, have also been investigated for the SLM process.

TABLE IV. Highest micro-hardness of SLM steel and iron-based alloys.

Material	Micro-hardness (HV)	References
Fe-Al intermetallic	800	83
Fe_3Al	353	68
Fe-Ni	232 (from 220 HB)	69
Fe-Ni-Cr	450	84
Fe-Ni-Cu-P	230	70
304L stainless steel	217	71
316L stainless steel	279	85
316L stainless steel	272 (from 104 HRB)	82
H20 tool steel	336 (from 34 HRC)	62
M2 high speed steel	900	86
Maraging steel	412 (from 42 HRC)	81
X110CrMoVAl 8-2 tool steel	493	63
Ultra high carbon steel	475	76

1. Applications

a. Medical and dental applications. Most research on titanium and its alloys is driven by its potential application as body prostheses or dental implants due to their biocompatibility. Moreover, they have high specific strength and elastic moduli closer to bone than Co-Cr alloys and stainless steel.[87] Research into titanium body implants has been done by several groups. Shiomi's group has built bone and dentals crowns using SLM cpTi.[88] Mullen's group investigated a unit-cell approach[89] and various scanning strategies[90] to make porous biocompatible constructs for orthopaedic applications using cpTi. Lin *et al.*[91] studied the structure and mechanical properties of a Ti64 cellular inter-body fusion cage, Murr *et al.*[92] focused their attention on the microstructure and mechanical properties of SLM Ti64 for biomedical applications and Warnke *et al.*[93] conducted cell experiments and showed that SLM Ti64 porous scaffolds allow total overgrowth of osteoblasts (bone cells). Vandenbroucke and Kruth[94] and Chen *et al.*[39] separately examined the dimensional accuracy of the SLM process for fabrication of dental frameworks. In some of the latest studies, Biemond *et al.*[95] examined the bone in-growth potential of trabecular-like implant surfaces produced by SLM of Ti64 in goats and concluded that the SLM produced parts showed good bone in-growth characteristics after 15 weeks. In Brazil, Jardini *et al.*[96] reported the use of EOSINT M270 system to fabricate titanium implant for a right cranio-maxillo-facial surgery. The custom-built implant fitted the patient well and allowed the surgery duration to be reduced due to pre-op planning with correct geometrical and anatomical details.

Furthermore, there were recent studies that seek to replace cpTi and Ti64 with other titanium based alloys. Chlebus *et al.*[97] studied the possibility of using Ti-6Al-7Nb for medical implants as it replaces vanadium with niobium in its chemical composition and this alloy has higher corrosion resistance and bio-tolerance compared to Ti64. Further studies on this novel titanium alloy were done by Marcu *et al.*[98] on endosseous implant and Dybala *et al.*[99] on cranio-maxillo-facial implants. Szymczyk *et al.*[100] also examined cultured cell growth of *Staphylococcus aureus* on Ti-6Al-7Nb scaffold and have demonstrated the potential of this titanium alloy in this application. SLM of Ti-24Nb-4Zr-8Sn has been examined by Zhang and Sercombe[101] as an improvement over Ti64 as a low modulus alloy. This would result in a reduced difference of moduli between implant and

surrounding bone, thus preventing bone resorption, which causes implant loosening. Zielinski *et al.*[102] presented Ti-13Zr-Nb as an alloy with better biocompatibility and longer lifetime for load-bearing implants. Speirs *et al.*[103] also studied another low modulus titanium alloy in Ti-13Nb-13Zr for medical applications.

b. Light weight structures and other applications. Besides allowing individualized medical implants to be built with low customization cost, SLM also enabled the fabrication of lightweight titanium scaffold structures for both medical and aeronautical applications. Wang *et al.*[104] fabricated cpTi porous structure by using a blend of TiH_2 and cpTi powders. Sun *et al.*[105] proposed an octahedral cell design for the construction of cell structure with SLM. Gorny *et al.*[106] characterized the deformation and failure behaviour and Brenne *et al.*[107] separately studied the uniaxial loading and bending load behaviour of SLM Ti64 porous structures. Xiao *et al.*[108] examined the compressive strength of high porosity (70%) lattice structures made of SLM titanium. Hasan *et al.*[109] studied the behaviour of SLM Ti64 micro-struts and proposed a heat treatment process to improve the properties of these structures. Mines *et al.*[58] tested the drop weight impact behaviour of sandwich structures with micro-lattice cores made via SLM of Ti64.

Besides applications in medical implants and light weight structures, SLM of Ti64 was first studied for fabrication of guidance section housing for the Sidewinder missile[110] and SLM of titanium has been investigated for fabrication of waveguide filters for radio frequency applications.[111] Caiazzo *et al.*[112] analysed the potential of SLM Ti64 in the production of aircraft engine turbine blade with internal channels or cavities which conventional manufacturing methods cannot achieve easily. In motorsports, Cooper *et al.*[113] reported that Red Bull Technology used laser AM technology to build thin wall hydraulic channels and examined how freedom of design would enable both component weight reduction and fluid flow improvement.

2. Properties

a. Relative density. SLM of titanium and titanium-based alloys has been very positive in terms of the relative density attained by various researchers. At early stages of research, Santos's group already achieved relative densities of 98% for cpTi.[114] Subsequent research works on titanium and titanium-based materials were able to achieve relative densities of 99.5% or higher. Table V summarizes the reported maximum density of the various SLM titanium materials.

b. Strength. Titanium parts fabricated by SLM display similar or superior strengths to their cast counter-parts. The UTS, YS, and respective elongation of the SLM titanium parts are tabulated in Table VI. UTS of the cast parts is also placed in the table for ease of comparison. SLM titanium alloys have higher or equal strength compared to their cast counterparts. This is due to the rapid solidification of very small amount of material that results in a more uniform chemical composition and microstructure throughout the component. Comparing Ti64 parts manufactured by Electron Beam Melting (EBM), where the UTS is about 1006 MPa,[118] SLM is able to produce components with higher UTS.

TABLE V. Highest reported relative density of SLM titanium.

Material	Highest relative density, %	References
cpTi	99.50	115
cpTi	99.90 (under vacuum)	116
Ti-6Al-4V	99.98	94
Ti-6Al-7Nb	99.95	97
Ti-24Nb-4Zr-8Sn	99.50	117

c. Surface roughness. There were few reported results on surface roughness of SLM titanium parts. Reference 114 reported a R_a of 3.96 μm for the top surface of laser AM Ti64 and Ref. 117 reported surface roughness of 5 μm for SLM cpTi.

d. Micro-hardness. Table VII shows the highest reported micro-hardness of the commercial pure titanium and titanium-based alloys fabricated by SLM. It is noted that high micro-hardness may not correspond to high relative density. For instance, in the SLM of Ti-6Al-4V, the highest micro-hardness of 613 HV corresponded to relative densities of 95.2% and 95.8%. However, samples with a higher relative density of 97.6% only gave a micro-hardness of 515 HW.[120]

C. Inconel and nickel-based alloys

After steel and titanium materials, nickel-based alloy is the most studied group of metals for the SLM process. Most of these publications are on Inconel, a family of nickel-based superalloys typically used in high-temperature applications. Nickel-based alloys studied for the SLM process include Inconel 625, Inconel 718, Chromel, Hastelloy X, Nimonic 263, IN738LC, and MAR-M 247. Many of these publications focus on the process parameters for formation of stable melt track since it is a pre-requisite of forming fully dense 3D components.

A particularly interesting nickel based material studied for the SLM process is the temperature-sensitive shape memory alloy (SMA) NiTi. It was first reported by Clare *et al.*[4] and they have managed to produce two-way trained NiTi with a relatively gradual phase transition. The SLM NiTi component exhibited a martensitic transition between 32 °C and 59 °C and an austenitic transition between 59 °C and 90 °C. Later, Meier *et al.* also published his work on SLM NiTi SMA and his results showed that the SLM component had high cyclic stability[121] but also slightly lower fracture strength and fracture strain compared to conventional NiTi.[122]

1. Applications

SLM of nickel-based superalloys, such as Inconel 718, has been studied for high temperature applications in aircraft engines as swirlers in combustion chambers, repair

TABLE VI. Highest reported tensile strengths of SLM titanium.

Material	UTS (MPa)	YS (MPa)	Elongation (%)	References	Material UTS (MPa)
cpTi	654	522	17.0	119	655
Ti-6Al-4V	1250	1125	6.00	94	1055
Ti-6Al-7Nb	1515	1440	1.40	97	1000
Ti-24Nb-4Zr-8Sn	665	563	13.8	117	…

patches,[123] gas turbine blades, and turbocharger rotors.[124] Inconel 718's excellent corrosion resistance and strength at high temperatures, fatigue resistance, wear resistance, and good weldability[125] have allowed it to be applied in these areas. In a review of manufacturing technologies for complex turbine blades by Lu *et al.*,[126] it was highlighted that Fraunhofer ILT and the MCP company had used SLM to produce turbine blades. These turbine blades had dense microstructure, high definition, and high surface quality. Moreover, a patent for manufacturing of a hollow turbine blade by SLM was applied for on 31 March 2011 in the USA.

Hastelloy X has high oxidation resistance and good high-temperature strength[127] and has possible applications in aircraft engines. Nimonic 263 is suitable for medium temperature structural applications and it has good fatigue properties and high oxidation resistance.[128] Rickenbacher *et al.*[129] also recommended IN738LC as a suitable material for heavy-duty gas turbine components. Combined with the advantages of SLM, such as freedom of design and high resolution, engine components can be made with complex internal structures to increase cooling efficiency or to reduce weight and bring about fuel savings for the airlines.

In addition to high-temperature related applications, SLM of nickel-based alloys has been studied for applications as die models for bevel gear[130] and porous filtration media.[64] Clare *et al.*[4] and Habijan *et al.*[131] studied the SLM of NiTi for potential applications in micro-electro-mechanical systems (MEMS) and smart carrier material for human mesenchymal stem cells (hMSC) to enhance bone growth and healing for critical bone defects, respectively.

2. Properties

a. Relative density. SLM Inconel 718, Hastelloy X, and Nimonic 263 have achieved near 100% relative density while there are room for improvement for SLM Inconel 625 and Chomel as shown in Table VIII.

b. Strength. Nickel-based alloys fabricated by SLM follow a similar trend to titanium-based alloys. They display higher UTS compared to their cast counterparts. Table IX shows the UTS, YS, and corresponding elongation of the SLM nickel-based alloys.

TABLE VII. Highest micro-hardness of SLM titanium.

Material	Micro-hardness (HV)	References
cpTi	308	116
Ti-6Al-4V	613	120
Ti-6Al-7Nb	464	97
Ti-24Nb-4Zr-8Sn	225	117

c. Surface roughness. There have been very few reports on the surface roughness of SLM nickel-based alloys. However, the reported figures have shown that these SLM parts have good surface roughness which is smaller than 10 μm. For instance, Mumtaz and Hopkinson[138] reported that surface roughness of SLM Inconel 625 can be as low as 4 μm for the top surface and Wang *et al.*[127] reported R_a of 6 μm with contour scanning.

d. Micro-hardness. In SLM nickel-based components, only a few reports on the micro-hardness can be found. It is shown that the micro-hardness can be improved by application of aging treatment. This can be shown by comparing the works of Wang *et al.* and Sanz and Navas as shown in Table X.

D. Other metals

Besides steel, titanium, and nickel, other metals, such as aluminium, copper, magnesium, cobalt-chrome, tungsten, and gold have also been studied for the SLM process. However, publications on each of these metals are significantly fewer. Hence, in this review, they are grouped together in this section.

Most of the works on SLM of aluminium alloys are based on AlSi10Mg, a common casting alloy. In a process optimization study conducted by Kempen *et al.*,[139] it was found that the quality of SLM component is dependent on powder morphology and content, besides the processing parameters. Small and spherical powders with higher silicon content gave a higher relative density in the SLM component than larger and irregularly-shaped powders. Other literatures on SLM of aluminium and its alloys also include pure aluminium, Al6061, AlSi12, and AlMg.

In the SLM of copper, there were early works on pure copper. Pogson *et al.*[140] attempted to process copper and H13 tool steel to make a multi-component mould tool with increased cooling rate. However, there was difficulty in

TABLE VIII. Highest reported relative density of SLM Inconel and nickel-based alloys.

Material	Highest relative density, %	References
Inconel 625	95.00	132–134
Inconel 718	99.98	135
Chomel	88.00	130
Hastelloy X	99.75	136
Nimonic 263	99.70	128

TABLE IX. Highest reported tensile strengths of SLM Inconel and nickel-based alloys.

Material	UTS (MPa)	YS (MPa)	Elongation (%)	References	Material UTS (MPa)
Inconel 625	1030	800	10.0	137	1000
Inconel 718	1148	907	25.9	125	1000
IN738LC	1184	933	8.40	129	1096
Hastelloy X	930.5	814	35.0	136	785
Nimonic 263	1085	818	24.0	128	940

preventing the embrittlement of the H13 tool steel by copper even with scanning speed as high as 400 mm/s. Due to copper's relatively low absorptivity to both Nd:YAG laser (63%) and CO_2 laser (32%) irradiation,[12] the energy consumption of the SLM process increased when fabricating copper parts. Moreover, the SLM of copper was also a challenge due to copper's high reactivity to atmospheric oxygen, even at low concentrations. Gu and Shen[141] addressed the issue of oxidation by using a copper-based powder mixture with 60 wt. % copper, 30 wt. % Cu10Sn, and 10 wt. % Cu8.4P. The additive phosphorus acted as a fluxing agent against oxidation of copper. SLM of other copper alloys, such as CuNi10, K220, and C18400, has also been published.

First paper on SLM of pure magnesium was published in 2010 by Ng's group[142] from The Hong Kong Polytechnic University. The challenge of processing magnesium with SLM comes from its high reactivity to oxygen and flammability. They approached this problem by building a SLM system containing a shielding box with circulating argon gas to lower the partial pressure oxygen level to less than 2 bars. However, their laser system had a maximum power of 28 W and they were only able to achieve single line melt tracks at a low scanning speed of 20 mm/s.

Tungsten has also been studied for the SLM process. Its high melting point of 3422 °C and low wettability presented a unique challenge for the SLM process. Tungsten is very hard and brittle, making it difficult to machine into complex shapes.[143] Fabricating tungsten alloys through conventional powder metallurgy is also costly as it requires expensive and dedicated tools. SLM provides a feasible alternative to processing of tungsten and widens its applications. SLM of pure tungsten and tungsten-nickel[144] alloys has also been examined.

Other metals, such as gold, silver, tantalum, and cobalt-chromium alloy, have also been reported in SLM literatures. However, journal publications on each of these metals are few and they are mostly focused on process optimization for these materials. Pauly *et al.*[145] presented SLM as a feasible processing technique for the production of bulk metallic glass due to the high cooling rate inherent in the process. Metallic glass has many desirable characteristics, such as near-theoretical strength, low Young's modulus, and high elasticity. Conventional methods have limited the shape of metallic glass to rods or ribbons, whereas SLM will be able to produce bulk metallic glass and widen its field of applications.

TABLE X. Highest micro-hardness of SLM Inconel and nickel-based alloys.

Material	Micro-hardness (HV)	References
Inconel 625	163 (from HRA)	133,134
Inconel 718	365	125
Inconel 718	470 (after aging treatment)	135
Chomel	740	130
Nimonic 263	370	128

1. Applications

a. Biomedical and dental applications. Cobalt-chrome has been studied by various groups for dental applications. Faure *et al.*[146] recorded results of 7000 dental elements produced over a span of 6 months. Averyanova *et al.*[147] studied the fabrication of 99% dense Co-Cr dental crown and bridges over a period of 14 months and concluded that SLM has good repeatability and these parts made by SLM meet the traditions standards. Oyague *et al.*[148] and Kim *et al.*[149] separately evaluated the fit of dental prostheses produced by SLM and reached different conclusions about the suitability of SLM technology in producing dental prostheses. In terms of hardness, elastic modulus, and strength, Ayyildiz *et al.*[150] concluded that SLM Co-Cr is suitable for dental applications. Bioactive and biodegradable magnesium orthopaedic implants by SLM have also been examined.[151]

b. Heat exchangers. One of the common applications for SLM copper is in the area of heat exchangers. This is due to copper's high thermal conductivity of 401 W/(m K). Pogson *et al.*[152] suggested that SLM of copper can be applied to micro heat-exchangers where wall thickness of about 100 μm is required. Becker[153] published an online article about tool inserts with internal cooling channels made from K220 copper alloy by SLM technology. Researchers have also tested SLM aluminium for heat transfer devices, such as heat sink[48] and arterial wick heat pipes.[154]

c. Other applications. Aluminium alloys have been tested for applications in waveguide filters alongside with SLM titanium.[111] Vilaro *et al.*[155] used SLM to build the water-pump of a race car to demonstrate the capability of SLM to create medium size parts. However, the water-pump has yet to be tested in a race car. Manfredi *et al.*[156] examined the possibility of creating lightweight structural parts for robotics applications and built a first finger exoskeleton.

Tungsten's high density, high melting temperature, and good corrosion resistance made it a suitable material for kinetic energy projectiles, radiation shielding, and mass balance in aircrafts.[157] The ability of SLM to manufacture micro-scale

structure also allowed Deprez *et al.*[158] to study tungsten as a magnetic resonance compatible multi-pinhole collimator.

SLM of precious metals, such as gold and silver, is of interest to the jewellery industry.[159] It allows the making of jewellery and ornaments with complex designs otherwise not feasible with conventional methods. Moreover, it helps to reduce the cost of production by out-phasing the use of expensive moulds and dies and by allowing unused powder to be reused for the next batch of production.[160]

2. Properties

a. Relative density. In terms of relative density, the figures attained for aluminium alloys and cobalt-chrome are above 96%. However, the relative densities range from 82% to 95% for other metals. Hence, there is still room for improvement in achieving near-full density parts for these metals. Table XI shows the highest reported relative density for each material processed by SLM.

b. Strength. The highest tensile strength reported for AlSi10Mg was 400 MPa, with a corresponding YS of 220 MPa and a breaking elongation of 11%.[162] There is little information about the UTS of other metals. This is probably because researchers have yet to produce near full-dense parts. High porosity usually means compromised internal structure, leading to a much lower strength and ductility. This is evident in the results reported by Sustarsic *et al.*, who obtained relatively low strength of 400 MPa for CuNi15 alloy with 92.00% relative density.[69]

c. Surface roughness. There are very few reports on the surface roughness of these metals produced by SLM. Calignano *et al.*[170] reported R_a of 14.35 μm for SLM AlSi10Mg. The surface roughness improved to 2.5 μm by shot-peening. Savalani *et al.* reported surface roughness of 20 μm for SLM magnesium parts[171] and Sustarsic *et al.* achieved R_a of 9 μm for CuNi15 alloy.[69]

d. Micro-hardness. Micro-hardness of SLM parts has been reported for some aluminium alloys, cobalt-chrome, magnesium, and gold. Jerrard *et al.*[161] found that hardness of the SLM part increased greatly when copper powder was added to the Al6061 powder at 30 wt. %. They have attributed this to the formation of $AlCu_2$ during the SLM process when these powders are mixed. Table XII shows the highest reported micro-hardness of the various SLM metals.

TABLE XI. Highest reported relative density of SLM aluminium, copper, magnesium, tungsten, gold, and cobalt-chrome.

Material	Highest relative density, %	References
Al6061	96.50	161
AlSi10Mg	99.50	162
Cu + Cu10Sn + Cu8.4P powder	84.00	163
Cu based powder	95.00	164
Cu10Sn + Cu8.4P + Ni	95.20	165
CuNi15	92.00	69
C18400	96.74	166
K220	99.90	167
Mg + 9 wt. % Al	82.00	168
Tungsten	89.92	158
24 Carat gold	89.60	169
CoCr	99.94	135

TABLE XII. Highest micro-hardness of SLM aluminium, copper, magnesium, gold, and cobalt-chrome.

Material	Micro-hardness (HV)	References
Al6061	50	161
Al6061 + 30 wt. % Cu	200	161
AlSi10Mg	149	162
CuNi15	116 (from 110 HB)	69
K220	192	167
Mg + 9 wt. % Al	75	168
24 Carat gold	29.3	159
CoCr	482	150

IV. CERAMICS

Ceramic materials studied for the SLM process included Li_2O-Al_2O_3-SiO_2 (LAS) glass, alumina (Al_2O_3), silica (SiO_2), yttria-stabilized zirconia (YSZ), tri-calcium-phosphate (TCP), alumina-zirconia mixtures, dental porcelain, alumina-silica mixture, silicon carbide, and silicon monoxide. In most of the experiments, CO_2 lasers ($\lambda \approx 10.6\,\mu$m) were used due to the higher absorptivity with ceramic materials. This is different from most experiments with metallic powders, where Nd:YAG or Yb:YAG ($\lambda \approx 1.06\,\mu$m) lasers were used. Although ceramic materials generally have a higher coupling efficiency with CO_2 lasers, Yap *et al.*[172] have shown that full melting of SiO_2 was still possible with Nd:YAG fibre laser. Their experiments on single track melting of SiO_2 resulted in glass-like rods with white SiO_2 powders adhering to the sides.

Generally, there are more challenges in the SLM of ceramics than that of metals. Ceramics are generally less dense than metals. Hence, ceramic powders have poor flowability, which does not allow a thin layer of ceramic powders to be spread evenly on the building platform. Nevertheless, Mapar *et al.*[173] improved the flowability of alumina-zirconia powder mixture by spray-drying and this allowed a thin layer to be deposited on to the building platform.

Furthermore, ceramics have a combination of high melting temperatures and low ductility. During the SLM process, a high energy input is required to increase the temperature to melting point. As the laser sweeps across the powder bed, the joint parts will experience high temperature fluctuation, creating high thermal stresses. Combined with the low ductility of ceramic materials, cracks can form. Wissenbach's research group overcame this problem by lowering the melting temperature and providing areal heating with a secondary CO_2 laser.

A. Applications

1. Medical and dental applications

Wissenbach's group has been working on SLM of ceramic materials for medical and dental applications. Wilkes

et al.[174] published papers on a SLM-produced dental restoration with zirconia and a bioresorbable bone substitute implant with TCP. Under light optical microscopy, the specimen was shown to be of high density but contained numerous cracks. TCP bone substitute implant was made by using alkaline borosilicate glass as binder. This allowed a lower melting temperature and kept TCP as the dominant phase in the part. However, the part was highly porous and had a low compressive strength of 8 MPa. Works on dental restoration bridge were reported by Hagedorn *et al*. who deployed a secondary laser as a source of pre-heating. However, the part built had poor surface finish with R_z of 150 μm.[175]

SLM also provides the capability to fabricate ceramic scaffolds. Liu[176] used silica solution-hydroxyapatite (HA) slurry to build bone scaffold for tissue engineering and evaluated its bioactivity with microculture tetrazolium test. The results concluded that the scaffold was suitable for cell culture and had potential for tissue engineering.

a. Other applications. Wang's group studied the laser melting of silica sand for applications in metal casting moulds.[177] The laser-melted parts had high porosity and rough surfaces. Hence, silicate infiltration was used as a post-process method to improve the density, strength, and surface roughness of the moulds. It was reported that the rapid casting process, enabled by direct laser sintering, provided a shorter and simpler alternative to conventional mould making and shortened the time required of the sand casting process.

Bertrand *et al*.[178] investigated the potential of SLM on yttria-zirconia by building thin wall structures, part of turbine blade, and nozzle. It was also suggested that SLM of alumina-zirconia can be applied to electrical or thermal insulation or wear resistant coating.[179]

B. Properties

1. Relative density

The inherent properties of ceramics make them challenging materials to fabricate with SLM. High melting temperatures and brittle nature of ceramics lead to crack formation when the parts undergo high temperature fluctuation during the process. Hence, achieving high relative density with ceramic materials is difficult as shown in Table XIII. Hagedorn *et al*. were able to achieve near full relative density by using a secondary laser for heating to reduce the temperature fluctuation of the SLM process.[27]

2. Strength

There is no report on the UTS or stress-strain behaviour of SLM ceramics. However, there are reports on the four-point bending strength (4PBS) and flexural strengths (FS) of SLM ceramics and these results are tabulated in Table XIV. Furthermore, Ref. 181 also reported a compressive strength of 15.5 MPa for direct laser sintered silica and Ref. 182 achieved 0.8 MPa for TCP.

TABLE XIII. Highest reported relative density of SLM ceramic materials.

Material	Highest relative density, %	References
ZrO_2-Y_2O_3	56	178
Al_2O_3-SiO_2	95	180
Al_2O_3-ZrO_2	100 (close to)	27
Silicate/hydroxyapatite	72	176

3. Surface roughness

The lowest reported figure for R_a of direct laser sintering or melting of ceramics is 19 μm.[181] Liu achieved R_a of 25 μm with silicate-HA mixture.[176] Hagedorn *et al*. deployed a secondary laser to solve the problem of crack formation and achieve high relative density. However, it also led high surface roughness. The reported R_z values were no lower than 150 μm.[175]

V. COMPOSITES

General interests in SLM of composite materials have caught on in the past few years. However, there are pioneering works in this area by Das *et al*. Their works involved nickel superalloy Mar-M-247, cobalt braze alloy Amdry 788, and boron nitride and aluminium oxide coated in titanium.[184] In most cases, SLM processing of composite materials involves melting a mixture of two or more type of powders, with one of the powder acting as the matrix material and the other as the reinforcing particle, usually a ceramic. For instance, titanium carbide (TiC) has been used with titanium and stainless steel to create SLM composite materials.

There were also research works that involved *in-situ* formation of reinforcement particles during the SLM process. Gu *et al*. carried out SLM for a powder mixture containing titanium powder and silicon nitride (Si_3N_4) with a composition molar ratio of 9:1. During the SLM process, an *in-situ* reaction took place: $9Ti + Si_3N_4 = 4TiN + Ti_5Si_3$. Microstructural analysis showed a Ti_5Si_3 matrix reinforced by granular TiN.[185] Their work displayed another possibility of the SLM process where the processed components had different compounds compared to the original powder material.

A. Applications

There are many applications of SLM composite materials, depending on the properties of the composite and the

TABLE XIV. Four-point bending strength and flexural strength of SLM ceramic materials.

Material	Four-point bending strength (4PBS) or flexural strength (FS) (MPa)	References
ZrO_2	9.79 (4PBS)	182
Al_2O_3-ZrO_2	500 (4PBS)	27
Silicate and hydroxyapatite	4.7 (4PBS)	176
Dental porcelain	31 (4PBS)	183
Al_2O_3-SiO_2	120 (FS)	180
Al_2O_3-ZrO_2	538.1 (FS)	174

demands of the applications. Most of the applications are in high value-added industries, such as aerospace, automotive, and medicine. Some research has been motivated by specific applications, such as heat resistant coating in engines,[186] load-bearing bone implants,[187] biodegradable implants,[188] and light-weight, high temperature structural materials.[189]

1. Medical implants

Hao *et al*. examined the SLM processing of HA and stainless steel for load bearing bone implants. This implant exploits the strength of steel and the ability of HA to stimulate bone and tissue re-growth at the interface of the implant and bone tissue in the human body.[187] Lindner *et al*. processed a high density, biodegradable composite material from β-tri-calcium phosphate and poly(D,L)-lactide reaching four-point bending strength of 23 MPa.[188] Shishkovskii *et al*. also experimented with HA and they processed it with NiTi. This material has the potential to function as porous implants or drug delivery system as NiTi has high strength, high corrosion resistance, biocompatibility, and a unique shape memory effect.[190] Polymer drug delivery systems built by SLS have been examined by Salmoria *et al*.[191] and current SLM technology will be able to produce metallic and composite counterparts.

2. Aerospace and automotive

For applications in the aerospace and the automotive industries, research has focused on high temperature performance and light-weight structures. Das *et al* used nickel based super alloy cermet to study the SLM production of abrasive turbine blade tips to minimize gas leakage and improve efficiency of gas turbines.[192] Mumtaz and Hopkinson[186] explored functionally graded zirconia reinforced Waspaloy™, a nickel based superalloy for high temperature applications, thermal structures, or heat resistant coating in engines. The functionally graded composite had layer-wise increasing concentration of zirconia from 0% to 10% and this would reduce the thermal coefficient mismatch between the substrate material and the thermal coating. Dadbakhsh *et al*.[193] focused on aluminium based metal matrix composites for aerospace and automotive applications to exploit the light-weight, high specific strength, and thermal conductivity of aluminium.

Gu *et al*. have studied titanium-based composites for intermediate and high temperature applications.[194] Titanium nitride (TiN)[195] and TiC (Ref. 189) reinforcements were added to titanium silicide (Ti_5Si_3) to improve its fracture toughness for high temperature structural applications. TiC reinforced titanium-aluminium matrix was also examined for intermediate temperature aerospace and power generation applications as the alloy matrix is lighter compared to modern nickel based superalloys.[196] SLM of pure titanium reinforced by TiC was also examined to increase its wear resistance for aerospace applications.[197]

3. Other applications

Gu also worked with Meiners[198] on SLM of tungsten-nickel-graphite powder mixture to attain *in situ* tungsten carbide (WC) reinforced $Ni_2W_4C(M_6C)$ for applications in machining tools and moulds with improved micro-hardness. Tungsten reinforced copper was explored by Li *et al*.[199] for applications in heavy duty electrical contacts, arcing resistance electrodes, and blocking material for microwave packages of microelectronic devices. The reinforced copper was reported to have superior thermal management properties and higher microwave absorption capacity.

B. Properties

1. Relative density

Reported relative densities of SLM composites range from 82% to 99.66% with an average of about 95%, as shown in Table XV.

2. Strength

Strength of SLM composite materials has been reported for a few early researches. However, the type of strength requirement varies according to the intended application. Besides the UTS, fracture toughness and four-point bending strength have also been reported for some SLM composite materials. For instance, Kim and Creasy obtained a fracture toughness of 95 MPa for Nylon 6 reinforced with clay nanoparticles.[208] Hon and Gill achieved UTS of 31 MPa for polyamide/SiC composite by using 50 wt.% SiC and laser energy density of 0.04 J/mm (Refs. 2 and 209). Hao *et al*. achieved UTS of 95 MPa for HA/stainless steel composite, adequately strong enough for loading bearing bone implant functions.[187] Gu and Shen attained UTS of 270 MPa for tungsten carbide-cobalt reinforced copper MMC.[210] Song *et al*. reported UTS of 764 MPa and YS of 302 MPa with silicon carbide reinforced iron matrix, highest of all composite materials reported thus far.[207] Lindner *et al*. reported a maximum four-point bending strength of 23 MPa for β-tricalcium phosphate/poly(D,L)-lactide composite intended for non-load bearing or low-load bearing implants.[188]

3. Micro-hardness and wear rate

Composite materials have improved hardness due to the inherent properties of the reinforcement materials. For tooling

TABLE XV. Highest reported relative density of SLM composite materials.

Material	Highest relative density, %	References
ZrO_2/Waspaloy™	99.66	186
TiC/Invar36	90.00	200
WC/$Ni_2W_4C(M_6C)$	96.30	198
WC/Ni	90.40	201
WC-Co/Cu	94.30	202
WC/Cu	95.70	203
β-tricalcium phosphate/poly(D,L)-lactide	98.00	188
TiC/Ti_5Si_3	96.90	189
FeO_3/AlSi10Mg	82.00	204
TiC/Ti	98.30	205
TiN/Ti_5Si_3	97.70	206
SiC/Fe	99.20	207

TABLE XVI. Highest reported micro-hardness of SLM composite materials.

Material	Micro-hardness (HV)	References
Hydroxyapatite/stainless steel	241.4	187
TiC/Invar36	380	200
WC/$Ni_2W_4C(M_6C)$	1870.9	198
WC/Ni	1292	201
WC-Co/Cu + 1 wt. % La_2O_3	401.8	212
WC/Cu	417.6	203
SiC/Fe	480	213
TiC/Ti_5Si_3	980.3	189
FeO_3/AlSi10Mg	165	204
TiC/Ti	577	205
TiN/Ti_5Si_3	1358	206

TABLE XVII. Lowest reported wear rates of SLM composite materials.

Material	Wear rate (mm^3/Nm)	References
TiC/Ti	1.8×10^{-7}	197
TiC/Ti_5Si_3	1.42×10^{-4}	189
TiN/Ti_5Si_3	6.84×10^{-5}	206
SiC/Al	0.65×10^{-4}	214

applications, high micro-hardness and low wear rates are desired. Gu and Zhang have worked on titanium based SLM composites to reduce the wear rate of the materials.[211] Table XVI and Table XVII show the micro-hardness and wear rates of the various SLM composite materials reported, respectively.

VI. SUMMARY AND REAEARCH TRENDS

This literature survey has shown that research in SLM has been mostly focused on metallic materials, with steel and titanium accounting for over half of all the publications from 1999 to 2014. The popularity of steel and titanium based materials is due to their applications in high value-added industries, such as aerospace and medicine. Figure 7 shows the compositional breakdown of the materials researched upon. Steel and titanium account for about 58% of all the research publications on SLM from 1999 to 2014. While ceramics and composite materials account for about 17% combined.

On a year-by-year basis, there is a general trend of continual increase in the number of publications from 1999 to 2014, with the exception of 2008. The dip corresponds with the decrease in revenues from various aspects of the AM sector as published by Wohlers Report 2015.[77] This could be caused by the 2008 global economic crisis. As most of the research works are on metallic materials, research on SLM of metallic materials follows a similar trend. In recent years, there are slight increases in the number of research publications on SLM of ceramics and composite materials. Figures 8(a) and 8(b) illustrate the trend of research for SLM and on the different types of materials. Within metallic materials, research in SLM of steel and iron-based alloys started early and has been the leading material in this field. Research interests in SLM of titanium rose sharply from 2010 as SLM titanium was found to be suitable for medical applications, such as load-bearing implants or light-weight prostheses. Interests in high-temperature super-alloys, such as Inconel and other metals, have also increased in recent years as shown by Figure 8(c).

Research on novel materials has increased in recent years. For instance, new titanium alloys, such as Ti6Al7Nb, have been examined to possibly replace the controversial Ti6Al4V due to its vanadium composition.[97] Ti24Nb4Zr8Sn (Ref. 117) and Ti13Nb13Zr (Ref. 103) have been studied to provide titanium alloys with low moduli to reduce moduli mismatch between the implant and surrounding bone tissue. There are also interests in metal matrix composites, where the composition can be easily modified by blending of different powders and smart materials, such as NiTi. Most recently, Pauly *et al*. have sparked the interests in SLM of bulk metallic glass, taking advantage of the high cooling rate in the SLM process.[145] Besides SLM of individual materials, there are also research works on SLM of multiple materials. In their review, Vaezi *et al*. highlighted the potential of SLM as a powder bed fusion for multi-material additive

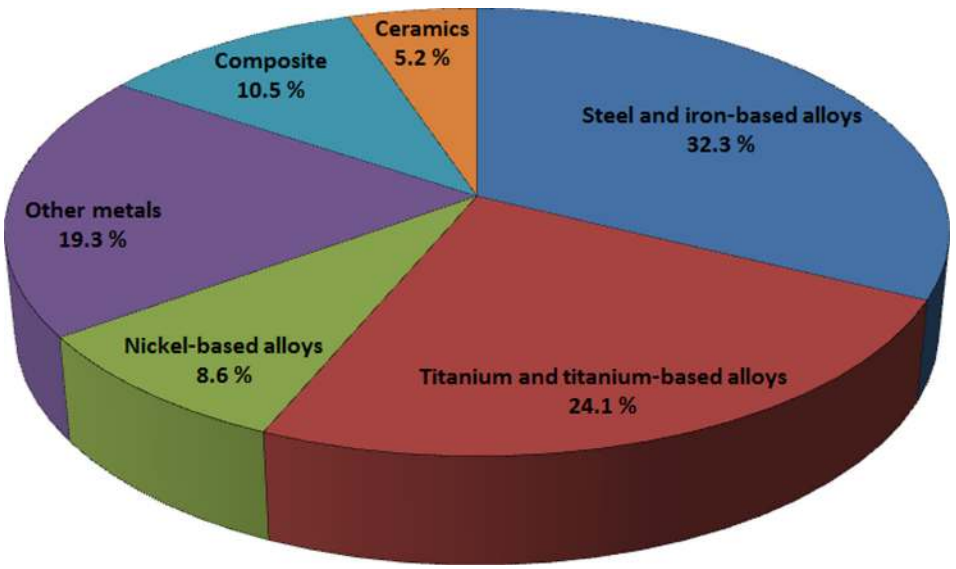

FIG. 7. Research publications on SLM of various materials. Data are based on research publications on SLM, LaserCusing, and DMLS indexed by Web of Science and ScienceDirect.

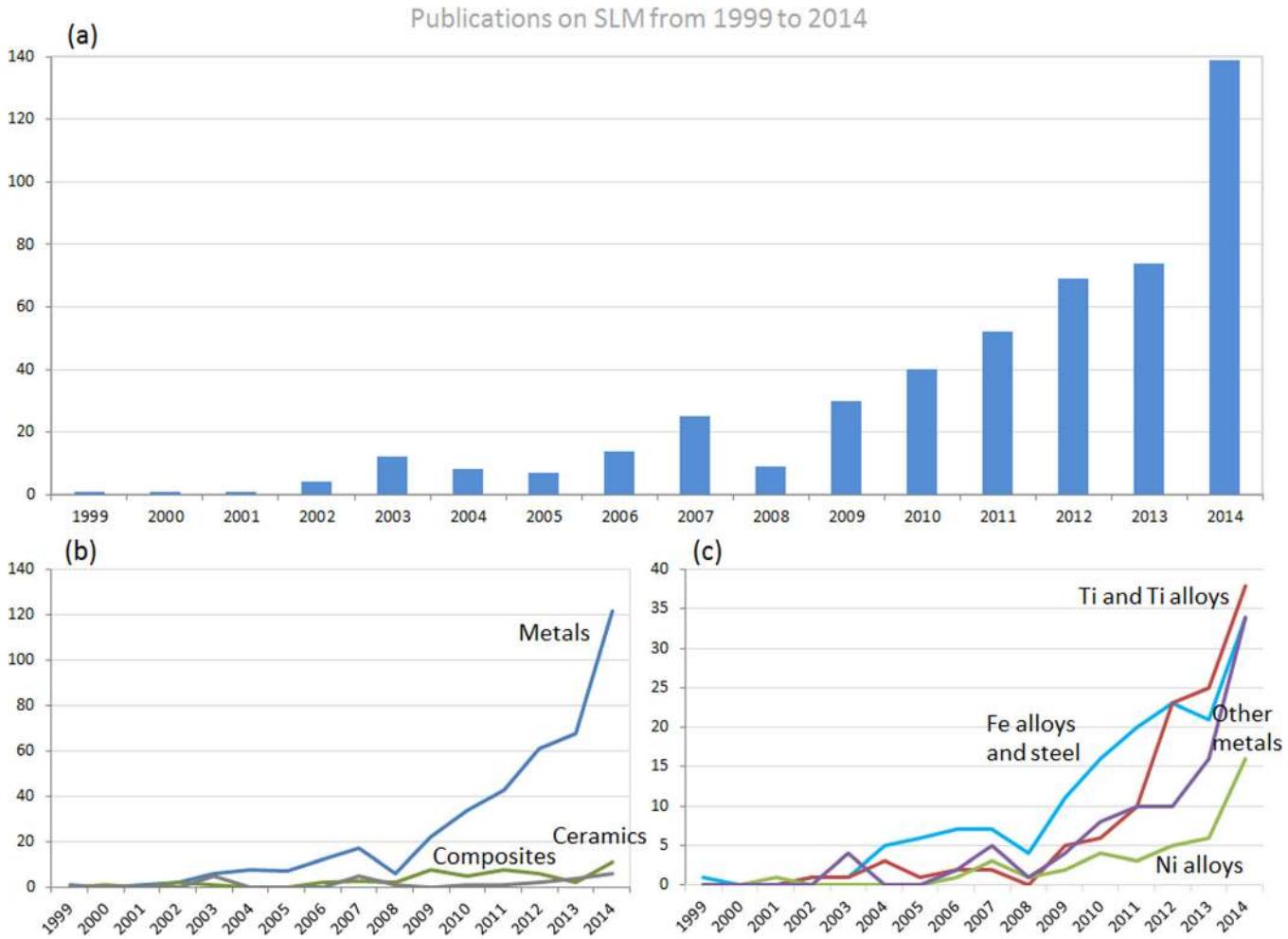

FIG. 8. (a) Research publications on SLM from 1999 to 2014. (b) Research publications on SLM of metals, ceramics, and composite materials. (c) Research publications on SLM between different metallic materials. Data are based on research publications on SLM, LaserCusing, and DMLS indexed by Web of Science and ScienceDirect.

manufacturing.[215] However, it also underlined the need for clever design of the material coating system to solve the problem of contamination. Liu *et al*. used SLM to join 316L stainless steel and copper (C18400) together and examined the interfacial characteristics.[216] They achieved this by creating a centre separator in the powder dispensing mechanism. The built part was found to have good metallurgical bonding at the interface between the two dissimilar metals.

In SLM, support structures are required for overhanging parts. These support structures function as anchors and heat sink to conduct excessive heat away. Hussein *et al*. examined the design of support structures with Ti6Al4V so as to reduce the required volume fraction for overhanging features during SLM process.[217] This would significantly reduce the amount of materials needed as support structure, reduce the time required for support removal, and laser scanning time required for support structure. It would also lower the cost of the SLM process as more powders can be reused for subsequent batches of production.

In addition to material development, there are also recent research works that focus on large powder-bed based AM equipment[218] and post-processing of SLM parts. Most of these post-processes aim at reducing residual thermal stresses, improving ductility and reducing surface roughness to meet the requirements of applications. They include various types of heat treatment, age-hardening, shot-peening, grinding, or polishing and these methods have been proven to be effective in improving the surface smoothness and reducing residual stresses.

In recent years, interests in direct part manufacturing for metals have increased. It is shown by the increase in global revenue for AM products and services, which quadrupled in the past five years, and that of AM metals that increased almost 50% in 2014 to USD 48.7 million. As of 2014, use of AM for direct part manufacturing takes up 42.6% of total products and services revenues from AM.[77] SLM offers a form of direct metal part production that is tool-less and capable of producing extremely complex shapes and geometrical features. This results in reduction in inventory and allows single consolidated parts to be built, that traditional manufacturing processes could only achieved by making a number of simple parts to be joint together.

In conventional manufacturing processes, it is common to have components designed with simple geometries to ease manufacturing. These designs are usually not optimized for their functions. With the geometric freedom offered by SLM,

components can be designed to the same functional specifications with less materials. In 2014, Airbus unveiled a cabin bracket optimized for weight saving without sacrificing functionality. With metal AM, Airbus aims to produce aircraft parts which weight 30%–55% less, while reducing raw material used by 90%.[219] The geometrical freedom in metal AM also allows for manufacturing of lattice structures for weight savings and designing of parts for improved fluid dynamics. For instance, Croft Filters, a manufacturer of bespoke filters, used SLM to produce new filters that only require one-step production. Conventionally, filter production involves cutting, welding, and lengthy labour processes.[220,221]

Besides the technical benefits of reduced tooling and freedom of design, SLM can also bring a change to the manufacturing sector in terms of economics. Together with the advancement in information technology and the internet, manufacturing can be decentralized. The economies of scale brought about by high-volume, centralized assembly lines are reduced.

However, there are still many challenges, besides legal concerns regarding copyrights, trade secret, patents, and government regulations as highlighted by Esmond and Phero *et al.*,[222] for SLM to be deemed mature and reliable for the industry to fully adopt it. The cost of materials and machines is high as producers, such as machine manufacturers tries to recoup investments in research and development. However, the unit price of machine is expected to decrease drastically when the machines are produced in larger volumes and when their related patents expire and market competition sets in. This is especially applicable for SLM, which the associated European patent was filed in 1998. The relatively low throughput and small build volume are also limitations that SLM has. In order to address this, SLM has developed the SLM 500 HL to double the build volume to 280 mm × 500 mm × 325 mm.

Given the market trend of direct part production via AM and increasing trend of research in the past decade, interests in SLM and similar technologies will continue to rise. The benefits brought about by SLM will further generate more applications that require direct part manufacturing. Hence, SLM is a technology that will stay relevant and important in the AM industry in the foreseeable future.

ACKNOWLEDGMENTS

The authors would like to acknowledge Interdisciplinary Graduate School, Nanyang Technological University for funding the Ph.D. studies.

[1]W. Meiners, K. D. Wissenbach, and A. D. Gasser, "Shaped body especially prototype or replacement part production," U.S. patent DE19649849C1 (1998).
[2]S. Das and J. J. Beaman, "Direct selective laser sintering of metals," U.S. patent US6676892B2 (2004).
[3]C. K. Chua and K. F. Leong, *3D Printing and Additive Manufacturing: Principles and Applications*, 4th ed. (World Scientific, Singapore, 2014), p. 518.
[4]A. T. Clare, P. R. Chalker, S. Davies, C. J. Sutcliffe, and S. Tsopanos, Int. J. Mech. Mater. Des. **4**, 181–187 (2007).
[5]R. Acharya, R. Bansal, J. J. Gambone, and S. Das, Metall. Mater. Trans. B **45**, 2247–2261 (2014).
[6]R. Acharya, R. Bansal, J. J. Gambone, and S. Das, Metall. Mater. Trans. B **45**, 2279–2290 (2014).
[7]R. Acharya, R. Bansal, J. J. Gambone, M. A. Kaplan, G. E. Fuchs, N. G. Rudawski, and S. Das, Adv. Eng. Mater. **17**, 942–950 (2015).
[8]R. Acharya and S. Das, Metall. Mater. Trans. A **46**, 3864–3875 (2015).
[9]R. Li, J. Liu, Y. Shi, L. Wang, and W. Jiang, Int. J. Adv. Manuf. Technol. **59**, 1025–1035 (2011).
[10]P. Krakhmalev and I. Yadroitsev, Intermetallics **46**, 147–155 (2014).
[11]S. Das, Adv. Eng. Mater. **5**, 701–711 (2003).
[12]N. K. Tolochko, Y. V. Khlopkov, S. E. Mozzharov, M. B. Ignatiev, T. Laoui, and V. I. Titov, Rapid Prototyping J. **6**, 155–161 (2000).
[13]P. Fischer, V. Romano, H. P. Weber, N. P. Karapatis, E. Boillat, and R. Glardon, Acta Mater. **51**, 1651–1662 (2003).
[14]X. Wang, T. Laoui, J. Bonse, J.-P. Kruth, B. Lauwers, and L. Froyen, Int. J. Adv. Manuf. Technol. **19**, 351–357 (2002).
[15]A. V. Gusarov and J. P. Kruth, Int. J. Heat Mass Transfer **48**, 3423–3434 (2005).
[16]L. E. Loh, Z. H. Liu, D. Q. Zhang, M. Mapar, S. L. Sing, C. K. Chua, and W. Y. Yeong, Virtual Phys. Prototyping **9**, 11–16 (2014).
[17]L.-E. Loh, C.-K. Chua, W.-Y. Yeong, J. Song, M. Mapar, S.-L. Sing, and D.-Q. Zhang, Int. J. Heat Mass Transfer **80**, 288–300 (2015).
[18]K. Mumtaz and N. Hopkinson, Rapid Prototyping J. **16**, 248–257 (2010).
[19]D. Bourell, A. B. Spierings, N. Herres, and G. Levy, Rapid Prototyping J. **17**, 195–202 (2011).
[20]B. Liu, R. Wildman, C. Tuck, I. Ashcroft, and R. Hague, in International Solid Freeform Fabrication Symposium: An Additive Manufacturing Conference (University of Texas at Austin, Austin, 2011), pp. 227–238.
[21]N. K. Tolochko, S. E. Mozzharov, I. A. Yadroitsev, T. Laoui, L. Froyen, V. I. Titov, and M. B. Ignatiev, Rapid Prototyping J. **10**, 78–87 (2004).
[22]J. P. Kruth, L. Froyen, J. Van Vaerenbergh, P. Mercelis, M. Rombouts, and B. Lauwers, J. Mater. Process. Technol. **149**, 616–622 (2004).
[23]K. Kempen, B. Vrancken, L. Thijs, S. Buls, J. Van Humbeeck, and J.-P. Kruth, in Solid Freeform Fabrication Symposium Proceedings, 2013, Austin, TX, USA (The University of Texas at Austin).
[24]I. Yadroitsev and I. Yadroitsava, Virtual Phys. Prototyping **10**(2), 67–76 (2015).
[25]M. Shiomi, K. Osakada, K. Nakamura, T. Yamashita, and F. Abe, CIRP Ann. **53**, 195–198 (2004).
[26]E. Yasa, J. Deckers, J.-P. Kruth, M. Rombouts, and J. Luyten, in *ASME 2010 10th Biennial Conference on Engineering Systems Design and Analysis* (ASME, 2010), pp. 695–703.
[27]Y.-C. Hagedorn, J. Wilkes, W. Meiners, K. Wissenbach, and R. Poprawe, Phys. Proc. **5**, 587–594 (2010).
[28]F. Abe, K. Osakada, M. Shiomi, K. Uematsu, and M. Matsumoto, J. Mater. Process. Technol. **111**, 210–213 (2001).
[29]G. Jandin, J. M. Bertin, L. Dembinski, and C. Coddet, *Manufacture of Stainless Steel Parts by Selective Laser Melting Process* (CRC Press, 2005), pp. 431–434.
[30]I. Tolosa, F. Garciandia, F. Zubiri, F. Zapirain, and A. Esnaola, Int. J. Adv. Manuf. Technol. **51**, 639–647 (2010).
[31]T. H. C. Childs, C. Hauser, and M. Badrossamay, CIRP Ann. **53**, 191–194 (2004).
[32]T. H. C. Childs, C. Hauser, and M. Badrossamay, Proc. Inst. Mech. Eng., Part B **219**, 339–357 (2005).
[33]T. H. C. Childs and C. Hauser, Proc. Inst. Mech. Eng., Part B **219**, 379–384 (2005).
[34]M. Badrossamay and T. H. C. Childs, Int. J. Mach. Tools Manuf. **47**, 779–784 (2007).
[35]P. G. E. Jerrard, L. Hao, and K. E. Evans, Proc. Inst. Mech. Eng., Part B **223**, 1409–1416 (2009).
[36]I. Yadroitsev, P. Bertrand, B. Laget, and I. Smurov, in *Annals of DAAAM for 2008 and Proceedings of the 19th International DAAAM Symposium* (DAAAM International, Vienna, 2008), pp. 1535–1536.
[37]J. P. Kruth, B. Vandenbroucke, J. Van Vaerenbergh, and I. Naert, Digital Manufacturing of Biocompatible Metal Frameworks for Complex Dental Prostheses by Means of SLS/SLM (Taylor & Francis, 2005), pp. 139–145.
[38]M. Wehmoller, P. H. Warnke, C. Zilian, and H. Eufinger, CARS: Computer Assisted Radiology and Surgery (Elsevier, 2005), pp. 690–695.
[39]G. X. Chen, X. Y. Zeng, Z. M. Wang, K. Guan, and C. W. Peng, *Equipment Manufacturing Technology and Automation* (Trans Tech Publications, 2011), Pts. 1–3, pp. 174–178.
[40]P. Bertrand and I. Smurov, in *International Conference on Lasers, Applications, and Technologies 2007: Laser-Assisted Micro- and*

Nanotechnologies (International Society for Optics and Photonics, 2007), p. H7320.
[41]Y. Q. Yang, J. B. Lu, Z. Y. Luo, and D. Wang, Rapid Prototyping J. **18**, 482–489 (2012).
[42]R. D. Li, J. H. Liu, Y. S. Shi, M. Z. Du, and Z. Xie, J. Mater. Eng. Perform. **19**, 666–671 (2010).
[43]R. Bibb, D. Eggbeer, P. Evans, A. Bocca, and A. Sugar, Rapid Prototyping J. **15**, 346–354 (2009).
[44]I. Yadroitsev, I. Yadroitsava, and I. Smurov, *Laser-Based Micro- and Nanopackaging and Assembly V* (International Society for Optics and Photonics, 2011).
[45]I. Yadroitsev, P. Bertrand, B. Laget, and I. Smurov, J. Nucl. Mater. **362**, 189–196 (2007).
[46]M. A. Garcia, C. Garcia-Pando, and C. Marto, *Conformal Cooling in Moulds With Special Geometry* (CRC Press, 2012), p. 409–412.
[47]J. J. Brandner, E. Hansjosten, E. Anurjew, W. Pfleging, and K. Schubert, *Laser-Based Micro- and Nanopackaging and Assembly* (International Society for Optics and Photonics, 2007), p. 45911.
[48]M. Wong, S. Tsopanos, C. Sutcliffe, and E. Owen, Rapid Prototyping J. **13**, 291–297 (2007).
[49]V. E. Beal, P. Erasenthiran, C. H. Ahrens, and P. Dickens, Proc. Inst. Mech. Eng., Part B **221**, 945–954 (2007).
[50]L. Wang, Q. S. Wei, Y. S. Shi, and P. J. Xue, Adv. Mater. Res. **502**, 67–71 (2012).
[51]B. Song, S. J. Dong, H. L. Liao, and C. Coddet, Mater. Res. Innovations **16**, 321–325 (2012).
[52]M. Santorinaios, W. Brooks, C. J. Sutcliffe, and R. A. W. Mines, *High Performance Structures and Materials III* (WIT Press, 2006), pp. 481–490.
[53]M. Smith, W. J. Cantwell, Z. Guan, S. Tsopanos, M. D. Theobald, G. N. Nurick, and G. S. Langdon, J. Sandwich Struct. Mater. **13**, 479–501 (2011).
[54]K. Ushijima, W. J. Cantwell, R. A. W. Mines, S. Tsopanos, and M. Smith, J. Sandwich Struct. Mater. **13**, 303–329 (2011).
[55]E. J. Harris, R. E. Winter, M. Cotton, M. Swan, and J. Maw, *Shock Compression of Condensed Matter—2011* (AIP, 2012), Pts. 1 and 2.
[56]Y. Shen, W. J. Cantwell, R. Mines, and K. Ushijima, *Materials and Manufacturing Technologies XIV* (Trans Tech Publications, 2012), pp. 386–391.
[57]Y. Shen, S. McKown, S. Tsopanos, C. J. Sutcliffe, R. A. W. Mines, and W. J. Cantwell, J. Sandwich Struct. Mater. **12**, 159–180 (2010).
[58]R. A. W. Mines, S. Tsopanos, Y. Shen, R. Hasan, and S. T. McKown, Int. J. Impact Eng. **60**, 120–132 (2013).
[59]O. Rehme and C. Emmelmann, J. Laser Micro Nanoeng. **4**, 128–134 (2009).
[60]Y. F. Shen, D. D. Gu, and P. Wu, Mater. Sci. Technol. **24**, 1501–1505 (2008).
[61]Z. Y. Wang, Y. F. Shen, and D. D. Gu, Powder Metall. **54**, 225–230 (2011).
[62]J. Milovanovic, M. Stojkovic, and M. Trajanovic, J. Sci. Ind. Res. **68**, 1038–1042 (2009).
[63]F. Feuerhahn, A. Schulz, T. Seefeld, and F. Vollertsen, *Lasers in Manufacturing* (Trans Tech Publications, 2013), pp. 836–841.
[64]I. Yadroitsev, I. Shishkovsky, P. Bertrand, and I. Smurov, Appl. Surf. Sci. **255**, 5523–5527 (2009).
[65]B. Song, S. Dong, S. Deng, H. Liao, and C. Coddet, Opt. Laser Technol. **56**, 451–460 (2014).
[66]M. Rombouts, J. P. Kruth, L. Froyen, and P. Mercelis, CIRP Ann. **55**, 187–192 (2006).
[67]B. Song, S. J. Dong, P. Coddet, H. L. Liao, and C. Coddet, Surf. Coat. Technol. **206**, 4704–4709 (2012).
[68]G. Rolink, S. Vogt, L. Senčekova, A. Weisheit, R. Poprawe, and M. Palm, J. Mater. Res. **29**, 2036–2043 (2014).
[69]B. Sustarsic, S. Dolinsek, M. Jenko, and V. Leskovšek, Mater. Manuf. Process. **24**, 837–841 (2009).
[70]Y. Wang, J. Bergstrom, and C. Burman, Mater. Sci. Eng., A **513–514**, 64–71 (2009).
[71]K. Abd-Elghany and D. L. Bourell, Rapid Prototyping J. **18**, 420–428 (2012).
[72]E. Yasa, J. Deckers, and J.-P. Kruth, Rapid Prototyping J. **17**, 312–327 (2011).
[73]C. S. Wright, M. Youseffi, S. P. Akhtar, T. H. C. Childs, C. Hauser, P. Fox, and J. Xie, *Advanced Materials Forum III* (Trans Tech Publications, 2006), Pts. **1** and 2, pp. 516–523.
[74]Z. H. Liu, D. Q. Zhang, C. K. Chua, and K. F. Leong, Mater. Charact. **84**, 72–80 (2013).
[75]C. Casavola, S. L. Carnpanelli, and C. Pappalettere, J. Strain Anal. Eng. Des. **44**, 93–104 (2009).
[76]M. A. Taha, A. F. Yousef, K. A. Gany, and H. A. Sabour, Materialwiss. Werkstofftech. **43**, 913–923 (2012).
[77]T. Wohlers, *Wohlers Report* (Wohlers Associates, 2015).
[78]K. Guan, Z. M. Wang, M. Gao, X. Y. Li, and X. Y. Zeng, Mater. Des. **50**, 581–586 (2013).
[79]H. K. Rafi, T. L. Starr, and B. E. Stucker, Int. J. Adv. Manuf. Technol. **69**, 1299–1309 (2013).
[80]A. B. Spierings, T. L. Starr, and K. Wegener, Rapid Prototyping J. **19**, 88–94 (2013).
[81]K. Kempen, E. Yasa, L. Thijs, J. P. Kruth, and J. Van Humbeeck, in *Lasers in Manufacturing 2011: Proceedings of the Sixth International Wlt Conference on Lasers in Manufacturing* (Elsevier, 2011), Vol. 12, Pt. A, pp. 255–263.
[82]J. Delgado, J. Ciurana, and C. A. Rodriguez, Int. J. Adv. Manuf. Technol. **60**, 601–610 (2012).
[83]B. Song, S. J. Dong, H. L. Liao, and C. Coddet, Int. J. Adv. Manuf. Technol. **69**, 1323–1330 (2013).
[84]A. Amanov, S. Sasaki, I. S. Cho, Y. Suzuki, H. J. Kim, and D. E. Kim, Mater. Des. **47**, 386–394 (2013).
[85]D. Wang, Y. Q. Yang, X. B. Su, and Y. H. Chen, Int. J. Adv. Manuf. Technol. **58**, 1189–1199 (2012).
[86]Z. H. Liu, C. K. Chua, K. F. Leong, K. Kempen, L. Thijs, E. Yasa, and J. P. Kruth, in 5th International Conference on Advanced Research in Virtual and Rapid Prototyping, 2011, Leiria, Portugal (CRC Press).
[87]F. Abe, E. C. Santos, Y. Kitamura, K. Osakada, and M. Shiomi, Proc. Inst. Mech. Eng., Part C **217**, 119–126 (2003).
[88]T. Laoui, E. Santos, K. Osakada, M. Shiomi, M. Morita, S. K. Shaik, and M. Takahashi, Proc. Inst. Mech. Eng., Part C **220**, 857–863 (2006).
[89]L. Mullen, R. C. Stamp, W. K. Brooks, E. Jones, and C. J. Sutcliffe, J. Biomed. Mater. Res., Part B **89B**, 325–334 (2009).
[90]R. Stamp, P. Fox, W. O'Neill, E. Jones, and C. Sutcliffe, J. Mater. Sci. Mater. Med. **20**, 1839–1848 (2009).
[91]C. Y. Lin, T. Wirtz, F. LaMarca, and S. J. Hollister, J. Biomed. Mater. Res., Part A **83A**, 272–279 (2007).
[92]L. E. Murr, S. A. Quinones, S. M. Gaytan, M. I. Lopez, A. Rodela, E. Y. Martinez, and R. B. Wicker, J. Mech. Behav. Biomed. Mater. **2**, 20–32 (2009).
[93]P. H. Warnke, T. Douglas, P. Wollny, E. Sherry, M. Steiner, S. Galonska, and S. Sivananthan, Tissue Eng., Part C **15**, 115–124 (2009).
[94]B. Vandenbroucke and J. P. Kruth, Rapid Prototyping J. **13**, 196–203 (2007).
[95]J. E. Biemond, G. Hannink, N. Verdonschot, and P. Buma, J. Mater. Sci. Mater. Med. **24**, 745–753 (2013).
[96]A. L. Jardini, M. A. Larosa, C. A. de Carvalho Zavaglia, L. F. Bernardes, C. S. Lambert, P. Kharmandayan, and R. Maciel Filho, Virtual Phys. Prototyping **9**, 115–125 (2014).
[97]E. Chlebus, B. Kuznicka, T. Kurzynowski, and B. Dybala, Mater. Charact. **62**, 488–495 (2011).
[98]T. Marcu, M. Todea, L. Maines, D. Leordean, P. Berce, and C. Popa, Powder Metall. **55**, 309–314 (2012).
[99]B. Dybala and E. Chlebus, *Titanium Scaffolds for Custom CMF Restorations* (ASME, 2013), pp. 517–520.
[100]P. Szymczyk, A. Junka, G. Ziolkowski, D. Smutnicka, M. Bartoszewicz, and E. Chlebus, Acta Bioeng. Biomech. **15**, 69–76 (2013).
[101]L. C. Zhang and T. B. Sercombe, *Powder Metallurgy of Titanium: Powder Processing, Consolidation and Metallurgy of Titanium* (Trans Tech Publications, 2012), pp. 226–233.
[102]A. Zielinski, S. Sobieszczyk, W. Serbinski, T. Seramak, and A. Ossowska, *Environmental Degradation of Engineering & Materials Engineering and Technologies* (Trans Tech Publications, 2012), pp. 225–232.
[103]M. Speirs, J. Van Humbeeck, J. Schrooten, J. Luyten, and J. P. Kruth, in *First CIRP Conference on Biomanufacturing* (Elsevier, 2013), pp. 79–82.
[104]Y. Wang, Y. F. Shen, Z. Y. Wang, J. L. Yang, N. Liu, and W. R. Huang, Mater. Lett. **64**, 674–676 (2010).
[105]J. F. Sun, Y. Q. Yang, and D. Wang, Mater. Des. **49**, 545–552 (2013).
[106]B. Gorny, T. Niendorf, J. Lackmann, M. Thoene, T. Troester, and H. J. Maier, Mater. Sci. Eng., A **528**, 7962–7967 (2011).

[107]F. Brenne, T. Niendorf, and H. J. Maier, J. Mater. Process. Technol. **213**, 1558–1564 (2013).
[108]D. M. Xiao, Y. Q. Yang, X. B. Su, D. Wang, and J. F. Sun, Biomed. Mater. Eng. **23**, 433–445 (2013).
[109]R. Hasan, R. Mines, and P. Fox, in 11th International Conference on the Mechanical Behavior of Materials, 2011, Villa Erba, Como, Italy (Elsevier).
[110]S. Das, M. Wohlert, J. J. Beaman, and D. L. Bourell, Mater. Des. **20**, 115–121 (1999).
[111]J. A. Lorente, M. M. Mendoza, A. Z. Petersson, L. Pambaguian, A. A. Melcon, and C. Ernst, *Single Part Microwave Filters Made From Selective Laser Melting* (IEEE, 2009), pp. 1421–1424.
[112]F. Caiazzo, F. Cardaropoli, V. Alfieri, V. Sergi, and L. Cuccaro, in 2012 XIX International Symposium on High-Power Laser Systems and Applications, 2013, Istanbul, Turkey (SPIE).
[113]D. E. Cooper, M. Stanford, K. A. Kibble, and G. J. Gibbons, Mater. Des. **41**, 226–230 (2012).
[114]E. C. Santos, K. Osakada, M. Shiomi, Y. Kitamura, and F. Abe, Proc. Inst. Mech. Eng., Part C **218**, 711–719 (2004).
[115]D. D. Gu, Y. C. Hagedorn, W. Meiners, G. B. Meng, R. J. S. Batista, K. Wissenbach, and R. Poprawe, Acta Mater. **60**, 3849–3860 (2012).
[116]B. C. Zhang, H. L. Liao, and C. Coddet, Vacuum **95**, 25–29 (2013).
[117]L. C. Zhang, D. Klemm, J. Eckert, Y. L. Hao, and T. B. Sercombe, Scr. Mater. **65**, 21–24 (2011).
[118]Y. Kok, X. Tan, S. B. Tor, and C. K. Chua, Virtual Phys. Prototyping **10**, 13–21 (2015).
[119]A. Barbas, A. S. Bonnet, P. Lipinski, R. Pesci, and G. Dubois, J. Mech. Behav. Biomed. Mater. **9**, 34–44 (2012).
[120]L. S. Bertol, W. Kindlein, F. P. da Silva, and C. Aumund-Kopp, Mater. Des. **31**, 3982–3988 (2010).
[121]H. Meier, C. Haberland, J. Frenzel, and R. Zarnetta, *Selective Laser Melting of NiTi Shape Memory Components* (CRC Press, 2010), pp. 233–238.
[122]H. Meier, C. Haberland, and J. Frenzel, *Structural and Functional Properties of NiTi Shape Memory Alloys Produced by Selective Laser Melting* (CRC Press, 2012), pp. 291–296.
[123]I. Kelbassa, P. Albus, J. Dietrich, and J. Wilkes, in Proceedings of the 3rd Pacific International Conference on Application of Lasers and Optics, 2008, Beijing, China (Laser Institute of America).
[124]K. N. Amato, S. M. Gaytan, L. E. Murr, E. Martinez, P. W. Shindo, J. Hernandez, and F. Medina, Acta Mater. **60**, 2229–2239 (2012).
[125]Z. Wang, K. Guan, M. Gao, X. Li, X. Chen, and X. Zeng, J. Alloys Compd. **513**, 518–523 (2012).
[126]Z. L. Lu, J. W. Cao, H. Jing, T. Liu, F. Lu, D. X. Wang, and D. C. Li, Virtual Phys. Prototyping **8**, 87–95 (2013).
[127]F. Wang, X. Wu, and D. Clark, Mater. Sci. Technol. **27**, 344–356 (2011).
[128]T. Vilaro, C. Colin, J. D. Bartout, L. Nazé, and M. Sennour, Mater. Sci. Eng., A **534**, 446–451 (2012).
[129]L. Rickenbacher, T. Etter, S. Hövel, and K. Wegener, Rapid Prototyping J. **19**, 282–290 (2013).
[130]K. Osakada and M. Shiomi, Int. J. Mach. Tools Manuf. **46**, 1188–1193 (2006).
[131]T. Habijan, C. Haberland, H. Meier, J. Frenzel, J. Wittsiepe, C. Wuwer, and M. Köller, Mater. Sci. Eng.,: C **33**, 419–426 (2013).
[132]S. Das, M. Wohlert, J. Beaman, and D. Bourell, in Proceedings to the Solid Freeform Fabrication Symposium, 1997, Austin, TX, USA (University of Texas at Austin).
[133]S. Das, J. J. Beama, M. Wohlert, and D. L. Bourell, Rapid Prototyping J. **4**, 112–117 (1998).
[134]S. Das, M. Wohlert, J. J. Beaman, and D. L. Bourell, J. Miner. Met. Mater. Soc. **50**, 17–20 (1998).
[135]C. Sanz and V. G. Navas, J. Mater. Process. Technol. **213**, 2126–2136 (2013).
[136]F. Wang, Int. J. Adv. Manuf. Technol. **58**, 545–551 (2011).
[137]I. Yadroitsev, A. Gusarov, I. Yadroitsava, and I. Smurov, J. Mater. Process. Technol. **210**, 1624–1631 (2010).
[138]K. Mumtaz and N. Hopkinson, Rapid Prototyping J. **15**, 96–103 (2009).
[139]K. Kempen, L. Thijs, E. Yasa, M. Badrossamay, W. Verheecke, and J. Kruth, "Process optimization and microstructural analysis for selective laser melting of $AlSi_{10}Mg$," in *Solid Freeform Fabrication Symposium*, 2011, University of Texas at Austin, Austin, TX, USA, pp. 484–495.
[140]S. Pogson, P. Fox, and W. O'Neill, "The effect of varying laser scanning speed on DMLR processed metal parts," in *Fourth National Conference on Rapid and Virtual Prototyping and Applications* (Professional Engineering Publications, Lancaster, UK, 2003), pp. 43–50.
[141]D. D. Gu and Y. F. Shen, Powder Metall. **49**, 258–264 (2006).
[142]C. C. Ng, M. M. Savalani, H. C. Man, and I. Gibson, Virtual Phys. Prototyping **5**, 13–19 (2010).
[143]D. Zhang, Q. Cai, and J. Liu, Mater. Manuf. Process. **27**, 1267–1270 (2012).
[144]D. Q. Zhang, Z. H. Liu, Q. Z. Cai, J. H. Liu, and C. K. Chua, Int. J. Refract. Met. Hard Mater. **45**, 15–22 (2014).
[145]S. Pauly, L. Löber, R. Petters, M. Stoica, S. Scudino, U. Kühn, and J. Eckert, Mater. Today **16**, 37–41 (2013).
[146]S. P. Faure, L. Mercier, P. Didier, R. Roux, J. F. Coulon, and S. Garel, Laser Sintering Process Analysis: Application to Chromium-Cobalt Alloys For Dental Prosthesis Production (ASME, 2012), pp. 9–15.
[147]M. Averyanova, P. Bertrand, and B. Verquin, Virtual Phys. Prototyping **6**, 179–185 (2011).
[148]R. C. Oyague, A. Sanchez-Turrion, J. F. Lopez-Lozano, J. Montero, A. Albaladejo, and M. J. Suarez-Garcia, Odontology **100**, 249–253 (2012).
[149]K. B. Kim, W. C. Kim, H. Y. Kim, and J. H. Kim, Dental Mater. **29**, E91–E96 (2013).
[150]S. Ayyildiz, E. H. Soylu, S. Ide, S. Kilic, C. Sipahi, B. Piskin, and H. S. Gokce, J. Adv. Prosthodontics **5**, 471–478 (2013).
[151]C. C. Ng, M. Savalani, and H. C. Man, Rapid Prototyping J. **17**, 479–490 (2011).
[152]S. Pogson, P. Fox, C. Sutcliffe, and W. O'Neill, Rapid Prototyping J. **9**, 334–343 (2003).
[153]D. Becker, "SLM components made from copper alloy powder open up new opportunities" (March 9, 2011).
[154]M. Ameli, B. Agnew, P. S. Leung, B. Ng, C. J. Sutcliffe, J. Singh, and R. McGlen, Appl. Therm. Eng. **52**, 498–504 (2013).
[155]T. Vilaro, S. Abed, and W. Knapp, in Proceedings of the 12th European Forum on Rapid Prototyping, 2008.
[156]D. Manfredi, F. Calignano, E. P. Ambrosio, M. Krishnan, R. Canali, S. Biamino, and C. Badini, Metall. Italiana **10**, 15–24 (2013).
[157]D. Zhang, Q. Cai, J. Liu, and R. Li, J. Mater. Eng. Perform. **20**, 1049–1054 (2010).
[158]K. Deprez, S. Vandenberghe, K. Van Audenhaege, J. Van Vaerenbergh, and R. Van Holen, Med. Phys. **40**, 012501 (2013).
[159]M. Khan and P. Dickens, Rapid Prototyping J. **18**, 81–94 (2012).
[160]J. Jhabvala, E. Boillat, and R. Glardon, Gold Bull. **44**, 113–118 (2011).
[161]P. Jerrard, L. Hao, S. Dadbakhsh, and K. Evans, in Proceedings of the 36th International MATADOR Conference (Springer, 2010), pp. 487–490.
[162]D. Buchbinder, H. Schleifenbaum, S. Heidrich, W. Meiners, and J. Bultmann, in Lasers in Manufacturing 2011: Proceedings of the Sixth International Wlt Conference on Lasers in Manufacturing (Elsevier, 2011), Vol. 12, Pt. A, pp. 271–278.
[163]D. Gu and Y. Shen, J. Mater. Process. Technol. **182**, 564–573 (2007).
[164]W. H. Wu, Y. Q. Yang, and Y. L. Huang, Chin. Opt. Lett. **5**, 37–40 (2007).
[165]D. D. Gu, Y. F. Shen, and Z. J. Lu, Mater. Des. **30**, 2099–2107 (2009).
[166]D. Zhang, Z. Liu, and C. Chua, in High Value Manufacturing: Advanced Research in Virtual and Rapid Prototyping: Proceedings of the 6th International Conference on Advanced Research in Virtual and Rapid Prototyping, Leiria, Portugal, 1–5 October 2013 (CRC Press, 2013), p. 285.
[167]D. Q. Zhang, Z. H. Liu, S. Li, M. Muzzammil, C. H. Wong, and C. K. Chua, *Selective Laser Melting: On The Study of Microstructure of K220* (Research Publishing, 2014), pp. 176–184.
[168]B. Zhang, H. Liao, and C. Coddet, Mater. Des. **34**, 753–758 (2012).
[169]M. Khan and P. Dickens, Gold Bull. **43**, 8 (2010).
[170]F. Calignano, D. Manfredi, E. P. Ambrosio, L. Iuliano, and P. Fino, Int. J. Adv. Manuf. Technol. **67**, 2743–2751 (2013).
[171]M. M. Savalani, C. C. Ng, and H. C. Man, *Selective Laser Melting of Magnesium for Future Applications in Medicine* (IEEE, 2010).
[172]C. Yap, C. Chua, Z. Dong, Z. Liu, and D. Zhang, in *High Value Manufacturing: Advanced Research in Virtual and Rapid Prototyping: Proceedings of the 6th International Conference on Advanced Research in Virtual and Rapid Prototyping, Leiria, Portugal, 1–5 October 2013* (CRC Press, 2013), p. 261.
[173]M. Mapar, D. Zhang, Z. Liu, W. Yeong, C. Chua, B. Tay, and F. Wiria, in *High Value Manufacturing: Advanced Research in Virtual and Rapid Prototyping: Proceedings of the 6th International Conference on*

Advanced Research in Virtual and Rapid Prototyping, Leiria, Portugal, 1–5 October 2013 (CRC Press, 2013), p. 267.
[174]J. Wilkes, Y. C. Hagedorn, W. Meiners, and K. Wissenbach, Rapid Prototyping J. **19**, 51–57 (2013).
[175]Y. C. Hagedorn, N. Balachandron, W. Meiners, K. Wissenbach, and R. Poprawe, in SFF Symposium, 2011, Austin, TX, USA (University of Texas at Austin).
[176]F.-H. Liu, J. Sol-Gel Sci. Technol. **64**, 704–710 (2012).
[177]X. H. Wang, J. Y. H. Fuh, Y. S. Wong, and Y. X. Yang, Int. J. Adv. Manuf. Technol. **21**, 1015–1020 (2003).
[178]P. Bertrand, F. Bayle, C. Combe, P. Goeuriot, and I. Smurov, Appl. Surf. Sci. **254**, 989–992 (2007).
[179]I. Shishkovsky, I. Yadroitsev, P. Bertrand, and I. Smurov, Appl. Surf. Sci. **254**, 966–970 (2007).
[180]P. Regenfuss, A. Streek, F. Ullmann, C. Kühn, L. Hartwig, M. Horn, and H. Exner, Interceramics **56**, 420–422 (2007).
[181]Y. Tang, J. Y. H. Fuh, H. T. Loh, Y. S. Wong, and L. Lu, Mater. Des. **24**, 623–629 (2003).
[182]J. Wilkes and K. Wissenbach, "Rapid manufacturing of ceramic components for medical and technical applications via selective laser melting," in *Euro-uRapid 2007 International User's Conference on Rapid Prototyping & Rapid Tooling & Rapid Manufacturing* (Fraunhofer, Frankfurt, Germany, 2007).
[183]X. Tian, B. Sun, J. G. Heinrich, and D. Li, Int. J. Adv. Manuf. Technol. **64**, 239–246 (2012).
[184]S. Das, N. Harlan, G. Lee, J. J. Beaman, D. L. Bourell, J. W. Barlow, and K. Sargent, Mater. Manuf. Process. **13**, 241–261 (1998).
[185]D. Gu, Y. Shen, and Z. Lu, Mater. Lett. **63**, 1577–1579 (2009).
[186]K. A. Mumtaz and N. Hopkinson, J. Mater. Sci. **42**, 7647–7656 (2007).
[187]L. Hao, S. Dadbakhsh, O. Seaman, and M. Felstead, J. Mater. Process. Technol. **209**, 5793–5801 (2009).
[188]M. Lindner, S. Hoeges, W. Meiners, K. Wissenbach, R. Smeets, R. Telle, and H. Fischer, J. Biomed. Mater. Res., Part A **97**, 466–471 (2011).
[189]D. Gu, Y.-C. Hagedorn, W. Meiners, K. Wissenbach, and R. Poprawe, Surf. Coat. Technol. **205**, 3285–3292 (2011).
[190]I. V. Shishkovskii, I. A. Yadroitsev, and I. Y. Smurov, Powder Metall. Metal Ceram. **50**, 275–283 (2011).
[191]G. V. Salmoria, P. Klauss, K. Zepon, L. A. Kanis, C. R. M. Roesler, and L. F. Vieira, Virtual Phys. Prototyping **7**, 107–115 (2012).
[192]S. Das, T. P. Fuesting, G. Danyo, L. E. Brown, J. J. Beaman, and D. L. Bourell, Mater. Des. **21**, 63–73 (2000).
[193]S. Dadbakhsh, L. Hao, P. G. E. Jerrard, and D. Z. Zhang, Powder Technol. **231**, 112–121 (2012).
[194]D. Gu, Y. Shen, and G. Meng, Mater. Lett. **63**, 2536–2538 (2009).
[195]D. D. Gu and Y. F. Shen, Acta Metall. Sin. **46**, 761–768 (2010).
[196]D. Gu, Z. Wang, Y. Shen, Q. Li, and Y. Li, Appl. Surf. Sci. **255**, 9230–9240 (2009).
[197]D. Gu, Y.-C. Hagedorn, W. Meiners, K. Wissenbach, and R. Poprawe, Compos. Sci. Technol. **71**, 1612–1620 (2011).
[198]D. Gu and W. Meiners, Mater. Sci. Eng., A **527**, 7585–7592 (2010).
[199]R. Li, Y. Shi, J. Liu, Z. Xie, and Z. Wang, Int. J. Adv. Manuf. Technol. **48**, 597–605 (2009).
[200]A. Gåård, P. Krakhmalev, and J. Bergström, J. Alloys Compd. **421**, 166–171 (2006).
[201]J. S. Chen, Y. H. Huang, X. S. Gao, B. Qiao, J. M. Yang, and Y. Q. He, Adv. Compos. Mater. **20**, 277–287 (2011).
[202]D. Gu and Y. Shen, Appl. Surf. Sci. **254**, 3971–3978 (2008).
[203]D. D. Gu and Y. F. Shen, J. Mater. Res. **24**, 3397–3406 (2009).
[204]S. Dadbakhsh and L. Hao, J. Alloys Compd. **541**, 328–334 (2012).
[205]D. Gu, G. Meng, C. Li, W. Meiners, and R. Poprawe, Scr. Mater. **67**, 185–188 (2012).
[206]D. D. Gu, C. Hong, and G. B. Meng, Metall. Mater. Trans. A **43A**, 697–708 (2012).
[207]B. Song, S. J. Dong, P. Coddet, G. S. Zhou, S. Ouyang, H. L. Liao, and C. Coddet, J. Alloys Compd. **579**, 415–421 (2013).
[208]J. H. Kim and T. S. Creasy, in *Solid Freeform Fabrication Symposium* (University of Texas at Austin, 2002), p. 224.
[209]K. K. B. Hon and T. J. Gill, CIRP Ann. **52**, 173–176 (2003).
[210]D. Gu and Y. Shen, Mater. Sci. Eng., A **435–436**, 54–61 (2006).
[211]D. Gu and G. Zhang, Virtual Phys. Prototyping **8**, 11–18 (2013).
[212]D. Gu, Y. Shen, L. Zhao, J. Xiao, P. Wu, and Y. Zhu, Mater. Sci. Eng., A **445–446**, 316–322 (2007).
[213]C. K. Srinivasa, C. S. Ramesh, and S. K. Prabhakar, Rapid Prototyping J. **16**, 258–267 (2010).
[214]S. K. Ghosh and P. Saha, Mater. Des. **32**, 139–145 (2011).
[215]M. Vaezi, S. Chianrabutra, B. Mellor, and S. Yang, Virtual Phys. Prototyping **8**, 19–50 (2013).
[216]Z. H. Liu, D. Q. Zhang, S. L. Sing, C. K. Chua, and L. E. Loh, Mater. Charact. **94**, 116–125 (2014).
[217]A. Hussein, L. Hao, C. Z. Yan, R. Everson, and P. Young, J. Mater. Process. Technol. **213**, 1019–1026 (2013).
[218]S. F. Wen, C. Z. Yan, Q. S. Wei, L. C. Zhang, X. Zhao, W. Zhu, and Y. S. Shi, Virtual Phys. Prototyping **9**, 213–223 (2014).
[219]Airbus. Printing the future: Airbus expands its applications of the revolutionary additive layer manufacturing process, 2014.
[220]N. Burns, Filtration + Separation **51**, 42–43 (2014).
[221]L. Nickels, "Meeting the mainstream," Metal Powder Report, Special Feature (2015).
[222]R. W. Esmond and G. C. Phero, Virtual Phys. Prototyping **10**, 9–12 (2014).